Group V secreted phospholipase A_2 plays a protective role against aortic dissection

Received for publication, April 4, 2020, and in revised form, May 22, 2020 Published, Papers in Press, June 1, 2020, DOI 10.1074/jbc.RA120.013753

Kazuhiro Watanabe[1,2], **Yoshitaka Taketomi**[2,3], **Yoshimi Miki**[2,3], **Kiyotaka Kugiyama**[1,4,*], **and Makoto Murakami**[2,3,4,5,*]

From the [1]*Department of Internal Medicine II, University of Yamanashi, Faculty of Medicine, Chuo, Yamanashi, Japan, the* [2]*Lipid Metabolism Project, Tokyo Metropolitan Institute of Medical Science, Tokyo, Japan, the* [3]*Laboratory of Microenvironmental and Metabolic Health Science, Center for Disease Biology and Integrative Medicine, Graduate School of Medicine, University of Tokyo, Tokyo, Japan,* [4]*AMED-CREST, Japan Agency for Medical Research and Development, Tokyo, Japan, and* [5]*FORCE, Japan Agency for Medical Research and Development, Tokyo, Japan*

Edited by Dennis R. Voelker

Aortic dissection is a life-threatening aortopathy involving separation of the aortic wall, whose underlying mechanisms are still incompletely understood. Epidemiological evidence suggests that unsaturated fatty acids improve cardiovascular health. Here, using quantitative RT-PCR, histological analyses, magnetic cell sorting and flow cytometry assays, and MS-based lipidomics, we show that the activity of a lipid-metabolizing enzyme, secreted phospholipase A_2 group V (sPLA$_2$-V), protects against aortic dissection by endogenously mobilizing vasoprotective lipids. Global and endothelial cell–specific sPLA$_2$-V–deficient mice frequently developed aortic dissection shortly after infusion of angiotensin II (AT-II). We observed that in the AT-II–treated aorta, endothelial sPLA$_2$-V mobilized oleic and linoleic acids, which attenuated endoplasmic reticulum stress, increased the expression of lysyl oxidase, and thereby stabilized the extracellular matrix in the aorta. Of note, dietary supplementation with oleic or linoleic acid reversed the increased susceptibility of sPLA$_2$-V–deficient mice to aortic dissection. These findings reveal an unexplored functional link between sPLA$_2$-driven phospholipid metabolism and aortic stability, possibly contributing to the development of improved diagnostic and/or therapeutic strategies for preventing aortic dissection.

Aortic dissection is a life-threatening condition that is caused by a tear in the intimal layer of the aorta or bleeding within the aortic wall, leading to the separation of the layers of the aortic wall. Two-thirds of such cases involve dissection of the thoracic ascending aorta, which is highly lethal (10–35%) even if emergency surgery can be performed at specialist centers (1–3). Although a key pathologic feature of aortic dissection is fragility of the aortic medial wall (3), the underlying mechanisms are still incompletely understood. Given that such dissection occurs suddenly without preceding clinical signs and that current treatment strategies are limited mainly to antihypertensive agents, biomarkers that can predict fragility and/or therapeutic targets for stabilization of the aortic wall are needed to improve patient outcomes (1–3).

This article contains supporting information.

* For correspondence: Kiyotaka Kugiyama, kugiyama@yamanashi.ac.jp; Makoto Murakami, makmurak@m.u-tokyo.ac.jp.

Although there are only limited opportunities for examining the pathogenesis of aortic dissection in patients who are seen after onset, several recent investigations using animal models have improved our understanding of the pathophysiology of this condition. It has been shown that aortic dissection can be induced by infusion of angiotensin II (AT-II), which raises blood pressure, into mice with an *ApoE*$^{-/-}$ genetic background, which develop extensive atherosclerosis characterized by an unusual plasma lipid profile (4, 5). However, considering that aortic dissection in humans is not accompanied by typical atherosclerotic plaques in many cases (6), studies of aortic dissection using *ApoE*$^{-/-}$ mice as a model system might not necessarily reflect all of the potential mechanisms, especially in terms of lipid metabolism.

Two main mechanisms underlying medial fragility of the aortic wall have been proposed: extracellular matrix (ECM) degradation and inflammation, where matrix metalloproteinases (MMPs) and pro-inflammatory cytokines contribute to the onset and severity of aortic dissection (3, 7). In humans, several ECM-related genes, such as *TGFB1*, *ACTA2*, and *COL3A1*, are associated with aortic dissection (3). Mutations in *LOX* (encoding lysyl oxidase (LOX), which is involved in cross-linking of the ECM proteins elastin and collagen) are also correlated with the condition, dissections of the thoracic ascending aorta being most common in affected patients (3, 8, 9). Indeed, administration of β-aminopropionitrile (BAPN), a LOX inhibitor; genetic deletion of tenascin-C, an ECM glycoprotein; or prolonged treatment with GM-CSF, a pro-inflammatory cytokine, in combination with AT-II infusion is able to induce various degrees of aortic dissection even in the absence of *ApoE* deletion (7, 10–12). Interestingly, a recent clinical study involving individuals with higher cardiovascular risks showed that the incidences of major cardiovascular events including aortic rupture were lower among those assigned to a Mediterranean diet supplemented with extra-virgin olive oil, which abundantly contains oleic acid (OA) and to a lesser extent linoleic acid (LA), than those assigned to a reduced-fat diet (12), suggesting a potentially beneficial role of these unsaturated fatty acids on cardiovascular health. However, considering that aortic dissection is an uncommon disease with a low incidence (5–30 cases/1 million people/year), the number of patients with this particular disease found in that study (12) might be too low to

precisely evaluate the efficacy of the OA/LA-rich diet on the disease conditions.

As well as being supplied exogenously as nutrients, unsaturated fatty acids are largely stored in membrane phospholipids and can be spatiotemporally released by phospholipase A_2 (PLA_2) enzymes. Among the PLA_2 enzymes identified to date, the secreted PLA_2 ($sPLA_2$) family comprises the largest subgroup, containing 10 catalytically active isoforms. Individual $sPLA_2$s show distinct tissue distributions and substrate preferences, thereby participating in diverse biological events in response to microenvironmental cues (13). $sPLA_2$s have been implicated in cardiovascular diseases, including atherosclerosis and aortic aneurysm, as the plasma levels of group IIA $sPLA_2$ ($sPLA_2$-IIA), a prototypic inflammatory $sPLA_2$, are correlated with atherosclerotic diseases (14–16), and genetic deletion of several $sPLA_2$s or treatment with varespladib, a pan-$sPLA_2$ inhibitor that broadly inhibits $sPLA_2$s in the group I/II/V/X branch, ameliorates atherosclerosis or aortic aneurysm in mice (17–22), although conflicting evidence also exists (23). Importantly, a phase III clinical trial employing varespladib for treatment of patients with cardiovascular diseases failed to demonstrate efficacy and in fact suggested an increased level of risk (24), raising the possibility that some $sPLA_2$s may have a protective rather than detrimental role in vascular diseases. Thus, the precise roles of $sPLA_2$s and underlying lipid metabolism in aortic diseases remain controversial, and no report has examined the contributions of $sPLA_2$s to aortic dissection.

In our continuing efforts to clarify the biological roles of $sPLA_2$s using various $sPLA_2$-knockout mouse strains in combination with comprehensive lipidomics (25–27), we herein show that mice lacking group V $sPLA_2$ ($sPLA_2$-V), which releases OA and LA preferentially (28, 29), frequently develop dissection in the thoracic ascending aorta, a feature that resembles aortic dissection in humans, shortly after AT-II infusion. $sPLA_2$-V is the major $sPLA_2$ isoform expressed in aortic endothelial cells (ECs), releasing OA and LA in response to AT-II stimulation and protecting against acute dissection of the thoracic ascending aorta in a manner dependent upon LOX-dependent ECM stabilization. We also show that the increased incidence of aortic dissection by endothelial $sPLA_2$-V deficiency could be rescued by dietary supplementation with OA or LA, providing a rationale for the beneficial role of these fatty acids for cardiovascular health.

Results

Expression of sPLA$_2$s in endothelial cells

Quantitative RT-PCR revealed that, among the nearly full set of $sPLA_2$s, *Pla2g2d, Pla2g2e, Pla2g3,* and *Pla2g5* (encoding $sPLA_2$-IID, -IIE, -III, and -V, respectively) were substantially expressed in the aorta of C57BL/6 mice (male, 8–12 weeks old), *Pla2g5* showing the highest expression (Fig. 1*A*). The expression level of *Pla2g5* in the aorta was almost equivalent to that in the heart (Fig. 1*B*), a tissue previously shown to express this $sPLA_2$ most abundantly (30, 31). The expression levels of *Pla2g5* in anatomically distinct aortas, including thoracic ascending, thoracic descending, and abdominal aortas, were almost equal (Fig. S1*A*). *Pla2g5* was also expressed in the inferior vena cava, where its expression level was less than half of that in the aortas (Fig. S1*A*). Immunohistochemical analysis showed that $sPLA_2$-V protein was localized mainly in the EC lining of the aorta (Fig. 1*C*) as well as in the myocardium (Fig. S1*B*) in *Pla2g5*$^{+/+}$ mice, whereas its staining was absent in *Pla2g5*$^{-/-}$ mice. To address the aortic expression of $sPLA_2$-V further, we isolated ECs from aortic tissues using anti-CD31 magnetic beads (Fig. 1*D*). Consistent with the immunohistochemistry (Fig. 1*C*), *Pla2g5* was expressed almost exclusively in the CD31-positive EC fraction (Fig. 1*E*). In contrast, the expression of *Pla2g2d* and *Pla2g3* in the CD31-positive EC fraction was far lower than that of *Pla2g5,* and that of *Pla2g2e* was distributed mainly in the CD31-negative non-EC fraction (Fig. 1*E*). Thus, $sPLA_2$-V is the major $sPLA_2$ expressed in aortic ECs in mice. As in mouse ECs, *PLA2G5* was the most abundant $sPLA_2$ isoform in human ECs (Fig. S1*C*), where its expression level was higher than that in human vascular smooth muscle cells (VSMCs) and fibroblasts (Fig. S1*D*).

Following AT-II infusion into mice (the procedure is illustrated schematically in Fig. 1*F*), the aortic expression of *Pla2g5* mRNA as well as mRNAs for the other three $sPLA_2$s (*Pla2g2d, Pla2g2e*, and *Pla2g3*) declined over 24–48 h (Fig. 1*G*). Confocal immunofluorescence microscopy confirmed that, prior to AT-II infusion, $sPLA_2$-V protein was distributed mainly in aortic ECs, being colocalized with the signature EC marker CD31, in *Pla2g5*$^{+/+}$ mice but not in *Pla2g5*$^{-/-}$ mice (Fig. 1*H*). Even after 48 h of AT-II infusion, at which time *Pla2g5* mRNA expression was reduced (Fig. 1*G*), $sPLA_2$-V protein was still present in the EC lining (Fig. 1*H*). Interestingly, the aortic staining of $sPLA_2$-V was nearly abolished after infusion of heparin into the circulation (Fig. 1*H*), suggesting that $sPLA_2$-V, a heparin-binding $sPLA_2$ (32), is largely retained on the luminal surface of the aortic endothelium through association with heparan sulfate proteoglycans.

Consistent with the reduced *Pla2g5* expression in the aortas of AT-II–infused mice (Fig. 1*G*), the expression of *PLA2G5* in human aortas obtained by curative resection from six patients with aortic dissection, all of whom had undergone aortic replacement, was significantly lower in dissecting sites than in nondissecting sites (Fig. 1*I*). Immunohistochemical analysis of the nondissecting site of a patient, where the histology of the aortic wall was maintained, showed that $sPLA_2$-V protein was localized mainly in ECs, which were also positive for CD31 in a serial section (Fig. 1*J*). Precise evaluation of $sPLA_2$-V immunostaining in the dissecting site was difficult because of the collapsed histology. Nonetheless, expression of *PLA2G5* was reduced in cultured human ECs after stimulation for 24 h with AT-II in a dose-dependent manner (Fig. S1*E*). Thus, although $sPLA_2$-V mRNA expression in ECs is decreased after AT-II treatment in both mice and humans, its protein expression is maintained on EC surfaces likely through binding to heparan sulfate proteoglycans.

Increased AT-II–induced thoracic aortic dissection in Pla2g5$^{-/-}$ mice

To clarify the roles of $sPLA_2$s in the pathophysiology of aortic dissection, we studied mice with knockout of the four $sPLA_2$s

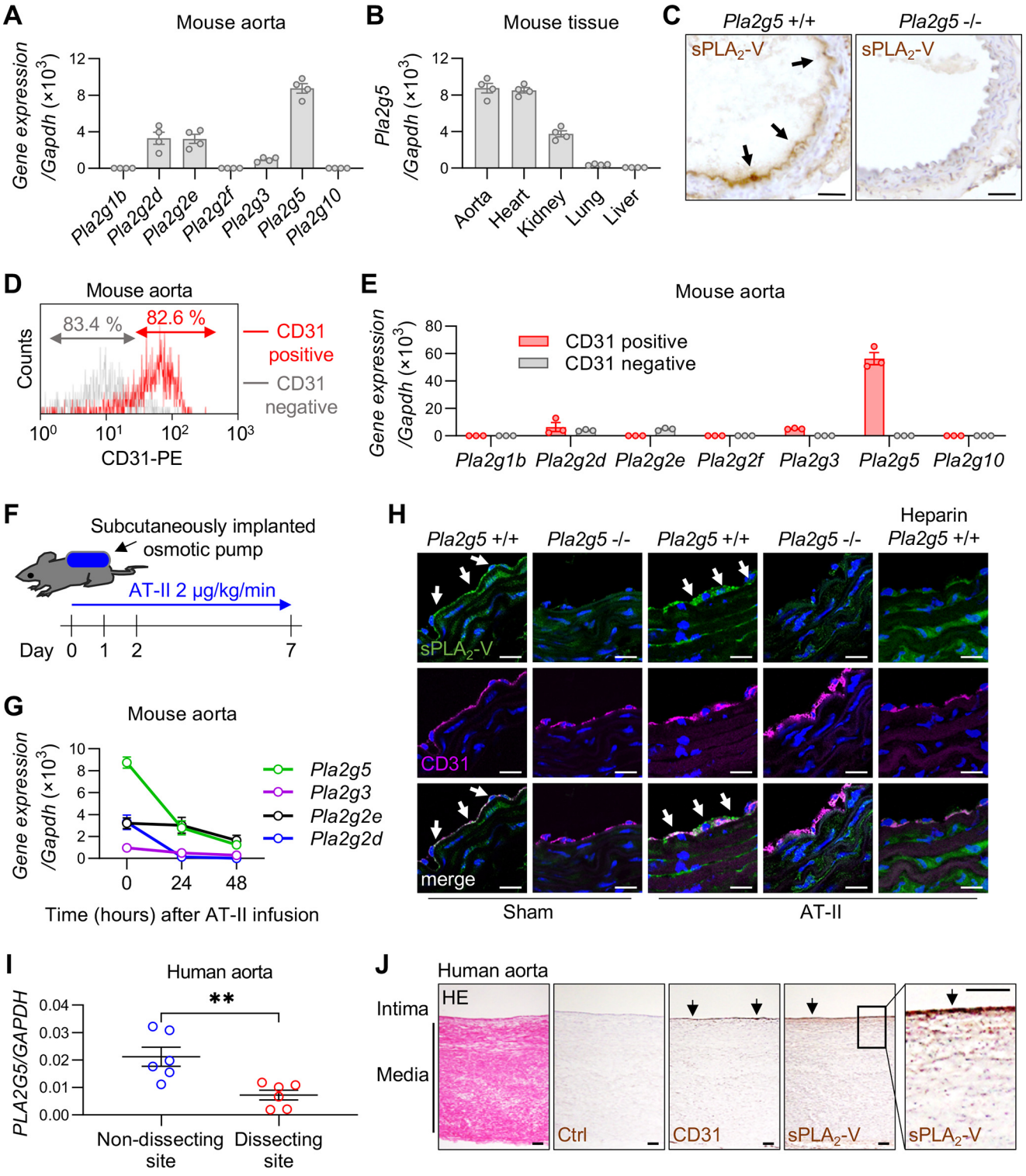

Figure 1. Expression of sPLA$_2$s in the aortas of mice and humans. *A*, expression of sPLA$_2$ mRNAs relative to *Gapdh* in the aorta of WT C57BL/6 mice ($n = 4$). *B*, expression of *Pla2g5* in various tissues of WT mice ($n = 4$). *C*, immunohistochemistry of sPLA$_2$-V in the aorta of *Pla2g5*$^{+/+}$ and *Pla2g5*$^{-/-}$ mice. *Arrows*, positive staining of sPLA$_2$-V. *Scale bars*, 100 μM. *D*, flow cytometry of CD31-positive/negative cells from WT mouse aorta. *E*, expression of sPLA$_2$ mRNAs of CD31 positive/negative cells from WT mouse aorta ($n = 3$). *F*, schematic procedure of AT-II infusion into mice using subcutaneously implanted osmotic pumps. *G*, time course of the expression of sPLA$_2$ mRNAs in WT mouse aorta after AT-II infusion ($n = 4$). *H*, immunofluorescence of sPLA$_2$-V (*green*) and CD31 (*magenta*) with DAPI (*blue*) in the aorta of *Pla2g5*$^{+/+}$ and *Pla2g5*$^{-/-}$ mice with or without AT-II infusion for 48 h. The *rightmost panels* represent the staining of *Pla2g5*$^{+/+}$ aorta after AT-II infusion, following perfusion with heparinized saline through the left ventricle before extraction. *Arrows* indicate positive staining of sPLA$_2$-V. *Scale bars*, 20 μM. *I*, expression of *PLA2G5* in nondissecting or dissecting site of human aorta ($n = 6$). **, $p < 0.01$ by unpaired *t* test. *J*, a representative section of human aorta stained with HE and immunohistochemistry of the serial sections with control IgG (*Ctrl*), anti-CD31 antibody, or anti-sPLA$_2$-V antibody. A *boxed area* is *magnified* on the *right*. *Arrows*, positive staining. *Scale bars*, 100 μM. Data are presented as mean ± S.E. (*error bars*) of the indicated number (*n*) of biological replicates.

that had been detected in the aorta. AT-II infusion has commonly been used to trigger aortic dissection in mice; however, these models typically require prolonged exposure to AT-II (>4 weeks) or use of elderly mice (>7 months old) or atherosclerosis-prone *ApoE*$^{-/-}$ mice, and the dissection takes place in the abdominal or thoracic descending, rather than thoracic ascending, aorta (4, 5, 33). Surprisingly, we found that *Pla2g5*$^{-/-}$ mice, even at a young age (8–12 weeks old), frequently developed aortic dissection after exposure to AT-II for a shorter period. Thus, when subjected to AT-II infusion only for 7 days, nearly half of *Pla2g5*$^{-/-}$ mice suffered from aortic dissection, which occurred mainly in the thoracic ascending aorta and often extended to the aortic arch (Fig. 2*A*). Some of the *Pla2g5*$^{-/-}$ mice died within 3 days due to rupture of the thoracic aorta, which was confirmed by an immediate autopsy showing intrathoracic hematoma accompanied by a tear of the aortic arch (Fig. 2*B*). Under the same conditions, only a few WT mice displayed a sign of aortic dissection, and none of them suffered sudden death due to aortic rupture. Histological examination of the lesions revealed dissection of the aortic wall with formation of intramural hematoma (as assessed by hematoxylin and eosin (HE) staining) and disruption of medial elastic fibers (as assessed by Elastica van Gieson (EVG) staining) in *Pla2g5*$^{-/-}$ mice (Fig. 2*C*). Thus, on day 7, the incidence of aortic dissection including rupture reached 44% (11 of 25) in *Pla2g5*$^{-/-}$ mice, whereas few or no aortic lesions were evident in *Pla2g2d*$^{-/-}$, *Pla2g2e*$^{-/-}$, *Pla2g3*$^{-/-}$, or their littermate WT mice (Fig. 2*D* and Fig. S2 (*A–C*)). Although hypertension is a main causal factor for aortic dissection and rupture, systolic and diastolic blood pressures as well as heart rates were similarly elevated in both *Pla2g5*$^{+/+}$ and *Pla2g5*$^{-/-}$ mice after 2 days of AT-II infusion (Fig. 2*E*), indicating that the increased incidence of aortic dissection caused by *Pla2g5* deficiency was due to a mechanism other than elevated blood pressure.

To elucidate the mechanism underlying the increased susceptibility of *Pla2g5*$^{-/-}$ mice to aortic dissection, we analyzed gene expression in the aortic tissues after 48 h of AT-II infusion, a time point just prior to dissection onset. Quantitative RT-PCR analysis of a panel of genes implicated in aortic stability, vascular remodeling, and inflammation showed that the AT-II–induced up-regulation of *Lox* mRNA, encoding a prototypic LOX that catalyzes the cross-linking of ECM proteins and thereby strengthens the aortic stability (34), was significantly attenuated in the aorta of *Pla2g5*$^{-/-}$ mice relative to *Pla2g5*$^{+/+}$ mice (Fig. 3*A*). In contrast, expression of mRNAs for other LOX family members (LOX-like proteins; encoded by *Loxl1–4*) and vascular remodeling markers (*Mmp2*, *Mmp9*, *Acta2*, *Col1a1*, *Col3a1*, and *Tgfb1*) was similar between *Pla2g5*$^{+/+}$ and *Pla2g5*$^{-/-}$ mice (Fig. 3*A*). The increased expression of proinflammatory cytokines (*Il1b*, *Il6*, and *Tnf*) in response to AT-II challenge was also not affected by *Pla2g5* deficiency (Fig. 3*A*). Kinetic studies showed that the aortic expression of *Lox* in *Pla2g5*$^{+/+}$ mice increased gradually over 48 h during AT-II infusion, whereas this response was significantly attenuated in *Pla2g5*$^{-/-}$ mice (Fig. 3*B*). AT-II–induced increases in aortic LOX protein expression (both the pro- and mature forms) (Figs. 3, *C* and *D*) and its activity (Fig. 3*E*) were also reduced in *Pla2g5*$^{-/-}$ mice relative to *Pla2g5*$^{+/+}$ mice. Moreover, elevation of the insoluble/soluble collagen ratio, which reflects an increase of collagen cross-linking by LOX, after AT-II infusion was lower in *Pla2g5*$^{-/-}$ mice than in *Pla2g5*$^{+/+}$ mice (Fig. 3*F*). After 48 h of AT-II infusion, immunofluorescence analysis using two different anti-LOX antibodies showed that LOX protein was increased mainly in medial VSMC layers beneath the CD31-positive EC layer in *Pla2g5*$^{+/+}$ mice, whereas the AT-II–induced LOX staining was attenuated in *Pla2g5*$^{-/-}$ mice (Fig. 3*G* and Fig. S2*D*). These results suggest that *Pla2g5* deficiency leads to aortic fragility due, at least in part, to reduced LOX induction in VSMCs and thereby insufficient ECM stability. Moreover, quantitative RT-PCR analysis using the aorta of aortic dissection patients (including samples of both dissecting and nondissecting sites) showed a positive correlation between *PLA2G5* and *LOX* expressions (Fig. 3*H*), implying human relevance. In contrast, aortic MMP activities as assessed by gelatin zymography were similar between *Pla2g5*$^{+/+}$ and *Pla2g5*$^{-/-}$ mice under both sham and AT-II infusion conditions (Figs. S2, *E* and *F*), suggesting that gelatinases, which can promote ECM degradation, did not profoundly affect the underlying phenotype.

Administration of BAPN, an inhibitor of LOX as well as its homologs LOXL1–4, into mice blocks ECM cross-linking within the vascular wall to trigger aortic dissection (35). Among the LOX members, LOX is the major isoform that is responsible for ~80% of total LOX activity in aortic VSMCs (36). Indeed, even without AT-II infusion, treatment with BAPN alone led to decreased survival of both *Pla2g5*$^{+/+}$ and *Pla2g5*$^{-/-}$ mice over 2–4 weeks due to aortic rupture (Fig. S3, *A–C*). Moreover, in the presence of BAPN, AT-II–induced dissection and rupture of the thoracic and abdominal aortas occurred similarly in both genotypes (Fig. S3, *D–F*), where the systolic and diastolic blood pressures as well as heart rates were similarly elevated in both *Pla2g5*$^{+/+}$ and *Pla2g5*$^{-/-}$ mice after AT-II infusion (Fig. S3*G*). Thus, the increased aortic instability in *Pla2g5*$^{-/-}$ mice relative to *Pla2g5*$^{+/+}$ mice was bypassed if LOX was pharmacologically inactivated, further supporting the notion that LOX may work downstream of sPLA$_2$-V to facilitate cross-linking of the ECM and thereby contribute to protection from aortic dissection.

Increased aortic dissection in EC-specific Pla2g5-null mice

To ascertain whether sPLA$_2$-V expressed in ECs is indeed responsible for aortic stability, mice carrying a floxed allele of *Pla2g5* (*Pla2g5*$^{flox/flox}$) were crossed with *Tie2-Cre* transgenic (Tg) mice to obtain mice lacking sPLA$_2$-V selectively in ECs (*Pla2g5*$^{flox/flox}$; *Tie2-Cre*) (Fig. 4*A*). Expression of *Pla2g5* in the aorta was blunted almost completely in *Pla2g5*$^{flox/flox}$; *Tie2-Cre* mice compared with control *Pla2g5*$^{flox/flox}$ mice (Fig. 4*B*), confirming that Cre-mediated recombination efficiently ablated *Pla2g5* expression in ECs. *Pla2g5* expression was also reduced by about 40% in the heart (Fig. 4*B*), probably because of its specific ablation in coronary arterial ECs, but not in other cells such as cardiomyocytes (37). Importantly, as in the case of global *Pla2g5*$^{-/-}$ mice (Fig. 3), *Pla2g5*$^{flox/flox}$; *Tie2-Cre* mice developed dissection of the thoracic aorta more frequently than control *Pla2g5*$^{flox/flox}$ mice within 7 days after the start of AT-II

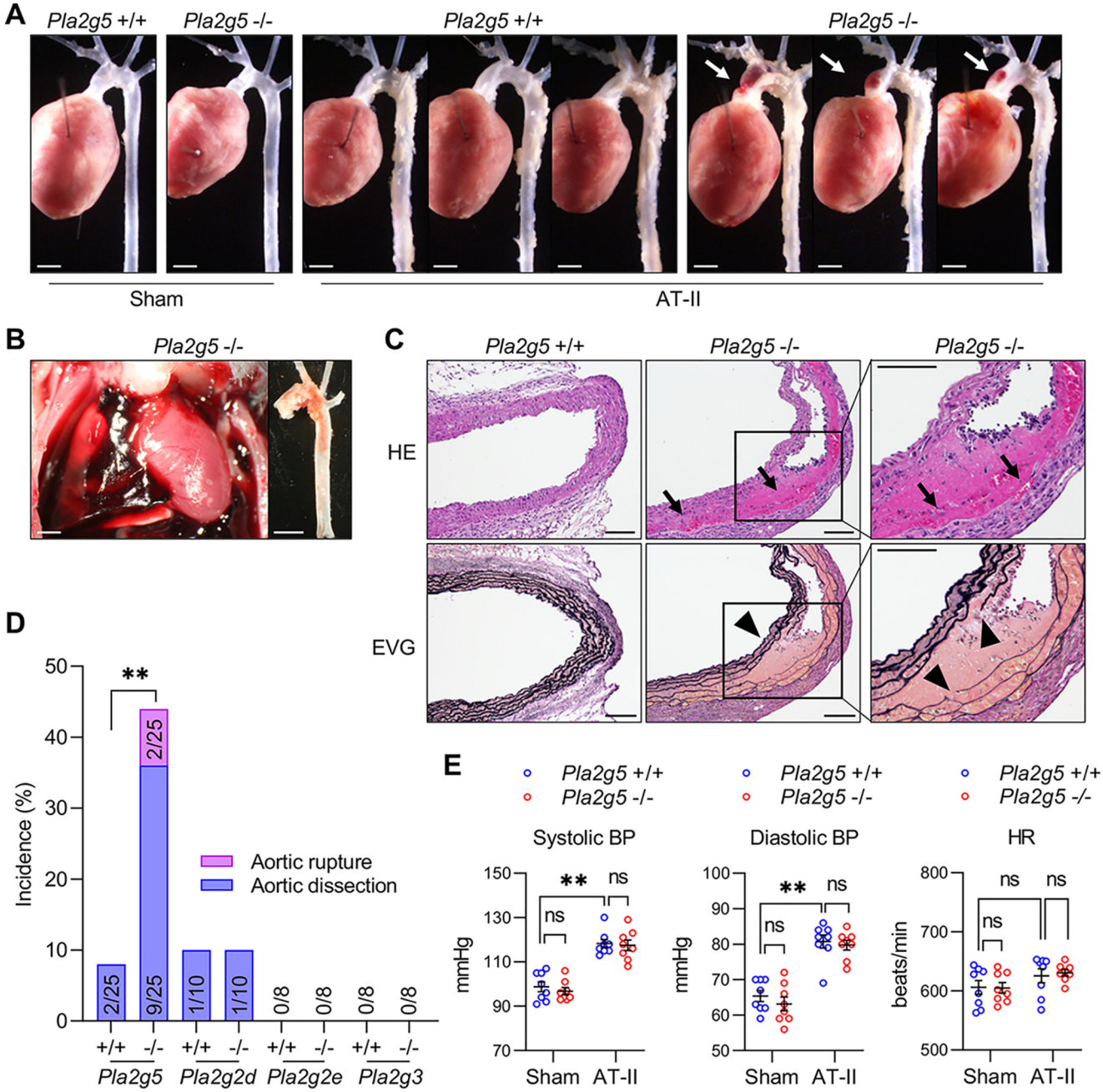

Figure 2. Increased AT-II-induced thoracic aortic dissection in *Pla2g5*$^{-/-}$ mice. *A*, representative thoracic aortas of *Pla2g5*$^{+/+}$ and *Pla2g5*$^{-/-}$ mice after 7 days of AT-II infusion or sham control. *Arrows* indicate aortic dissection with intramural hematoma. *Scale bars*, 1 mm. *B*, representative intrathoracic hematoma and ruptured thoracic aorta of a *Pla2g5*$^{-/-}$ mouse after 3 days of AT-II infusion. *Scale bars*, 1 mm. *C*, representative sections of the thoracic aorta of *Pla2g5*$^{+/+}$ and *Pla2g5*$^{-/-}$ mice stained with HE or EVG. *Arrows* indicate intramural hematoma, and *arrowheads* indicate dissection of the aortic wall accompanied by elastin fragmentation. *Scale bars*, 100 μM. *Boxes* are magnified on the *right*. *D*, incidence of thoracic aortic dissection or rupture in *Pla2g5*$^{-/-}$ ($n = 25$), *Pla2g2d*$^{-/-}$ ($n = 10$), *Pla2g2e*$^{-/-}$ ($n = 8$), *Pla2g3*$^{-/-}$ ($n = 8$), and littermate WT mice within 7 days of AT-II infusion. **, $p < 0.01$ by Fisher's exact test. *E*, systolic blood pressure (*BP*), diastolic blood pressure, and heart rate (*HR*) of *Pla2g5*$^{+/+}$ and *Pla2g5*$^{-/-}$ mice with or without AT-II infusion for 2 days ($n = 8$). **, $p < 0.01$; *ns*, not significant by two-way ANOVA with Tukey's multiple-comparison test. Data are presented as mean ± S.E. of the indicated number (*n*) of biological replicates.

administration (Fig. 4, *C* and *D*). In addition, the induction of LOX at the mRNA (Fig. 4*E*), protein (Figs. 4, *F* and *G*), and activity (Fig. 4*H*) levels in the aorta after 48 h of AT-II infusion was significantly attenuated in *Pla2g5*$^{flox/flox}$; *Tie2-Cre* mice relative to *Pla2g5*$^{flox/flox}$ mice. Expression levels of neither other LOX family members, vascular remodeling markers, nor inflammatory markers were affected by *Pla2g5* deficiency (Fig. 4*E* and Fig. S4). After 48 h of AT-II infusion, immunofluorescence analysis showed that LOX protein was increased mainly in medial VSMC layers beneath the CD31-positive EC layer in *Pla2g5*$^{flox/flox}$ mice, whereas the AT-II–induced LOX staining was attenuated in *Pla2g5*$^{flox/flox}$; *Tie2-Cre* mice (Fig. 4*I*). Thus, EC-specific deletion of sPLA$_2$-V largely recapitulates its global deficiency. Taken together, these results suggest that sPLA$_2$-V expressed in ECs has a protective role against AT-II–induced aortic dissection at least partly through increased expression of LOX in the aortic tissue.

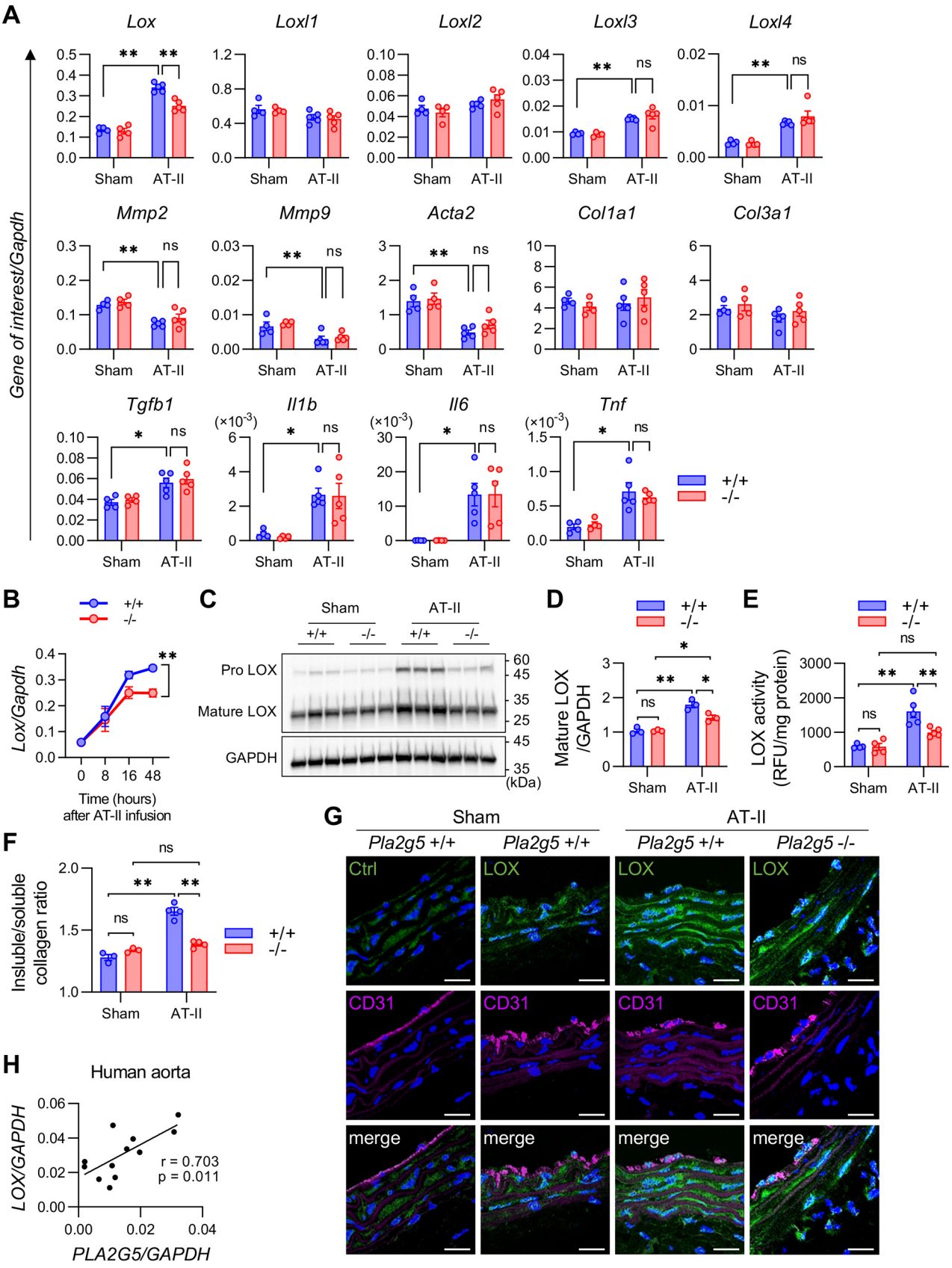
A
Lox
Loxl1
Loxl2
Loxl3
Loxl4
Mmp2
Mmp9
Acta2
Col1a1
Col3a1
Tgfb1
Il1b
Il6
Tnf
Gene of interest/Gapdh
Sham
AT-II
+/+
-/-
B
Lox/Gapdh
Time (hours) after AT-II infusion
C
Pro LOX
Mature LOX
GAPDH
(kDa)
D
Mature LOX /GAPDH
E
LOX activity (RFU/mg protein)
F
Insluble/soluble collagen ratio
G
Pla2g5 +/+
Pla2g5 -/-
Ctrl
LOX
CD31
merge
H
Human aorta
LOX/GAPDH
PLA2G5/GAPDH
r = 0.703
p = 0.011

Altered lipid profiles in Pla2g5$^{-/-}$ mice after AT-II infusion

Because sPLA$_2$-V is a phospholipase, we reasoned that the aortic protection by sPLA$_2$-V may involve some lipids mobilized by this enzyme. To identify such lipids (fatty acids, lysophospholipids, and their metabolites) that are potentially mobilized by sPLA$_2$-V in mouse aorta, we performed lipidomics analysis by LC coupled with electrospray ionization-tandem MS (ESI-MS/MS) using aortic tissues after 12 h of AT-II infusion, at which time *Pla2g5* expression was still high (Fig. 1*G*) and *Lox* expression was apparently increased (Fig. 3*B*) in *Pla2g5*$^{+/+}$ mice.

A heat map summary of overall changes in free fatty acids, lysophospholipids, and their metabolites is shown in Fig. 5 (*A–C*), and quantitative values of the representative metabolites are shown in Fig. 5 (*D–G*). We found that OA (18:1) and LA (18:2) were markedly elevated in the aorta of *Pla2g5*$^{+/+}$ mice following AT-II challenge, whereas these increases occurred only minimally in that of *Pla2g5*$^{-/-}$ mice (Figs. 5, *A* and *D*). Among the highly unsaturated fatty acids (HUFAs), including arachidonic acid (AA; 20:4), eicosapentaenoic acid (EPA; 20:5), and docosahexaenoic acid (DHA; 22:6), which were much less abundant than OA and LA, AA was also significantly reduced in AT-II–infused *Pla2g5*$^{-/-}$ mice relative to *Pla2g5*$^{+/+}$ mice (Fig. 5, *A* and *D*). Likewise, several lysophospholipid species, including lysophosphatidylcholine (LPC), lysophosphatidylethanolamine (LPE) and to a lesser extent lysophosphatidic acid (LPA), lysophosphatidylinositol (LPI), and lysophosphatidylserine (LPS), all of which had an unsaturated or monounsaturated fatty acyl chain representing typical PLA$_2$ reaction products, were also elevated in AT-II-treated *Pla2g5*$^{+/+}$ mice, whereas these changes of lysophospholipids were substantially lower in *Pla2g5*$^{-/-}$ mice (Fig. 5, *B* and *E*). Although aortic expression of *Pla2g4a* (encoding cytosolic PLA$_2\alpha$ (cPLA$_2\alpha$), a central regulator of AA release) was increased following AT-II infusion, it was not affected by the absence of sPLA$_2$-V (Fig. S5*A*). These results suggest that sPLA$_2$-V mobilizes OA and LA (and to a much lesser extent AA) from phosphatidylcholine (PC) and phosphatidylethanolamine (PE) in AT-II–stimulated, rather than unstimulated, aortic cells, being apparently consistent with the properties of this enzyme already reported in several other systems (28, 29, 38). Plasma levels of fatty acids and lysophospholipids were not affected by *Pla2g5* deficiency regardless of AT-II infusion (Fig. S5, *B* and *C*). Among the HUFA metabolites, AT-II treatment increased the aortic production of several AA metabolites and related eicosanoids, among which only prostaglandin E$_2$ (PGE$_2$) was significantly lower in *Pla2g5*$^{-/-}$ mice than in *Pla2g5*$^{+/+}$ mice (Fig. 5, *C* and *F*). In addition, lipoxin A$_4$ (LXA$_4$, an anti-inflammatory AA metabolite), as well as several metabolites in the 12/15-lipoxygenase pathway (12- and 15-hyrdroxytetraenoic acids (HETEs)), tended to be increased in AT-II–infused *Pla2g5*$^{-/-}$ mice relative to *Pla2g5*$^{+/+}$ mice (Fig. 5, *C* and *G*), with concomitant increases in the expression of *Alox12* and *Alox15* (encoding 12- and 15-lipoxygenases, respectively) (Fig. S5*D*), which might reflect a secondary effect of aortic alterations caused by *Pla2g5* deficiency.

We also monitored plasma lipoproteins and exosomes, whose phospholipids are potential targets of sPLA$_2$-V, in *Pla2g5*$^{+/+}$ and *Pla2g5*$^{-/-}$ mice. Although sPLA$_2$-V alters the lipoprotein profile by cleaving OA- or LA-containing PC in LDL after its induction in hypertrophic adipocytes during obesity (28), the lipoprotein composition under normal dietary conditions was unaffected by *Pla2g5* deficiency regardless of AT-II infusion (Fig. S5*E*). AT-II infusion increased the protein content and the number of plasma exosomes and decreased their sizes (Fig. S6, *A–C*). Although sPLA$_2$-V is capable of hydrolyzing microvesicle membranes *in vitro* (39), plasma exosomes (in terms of protein content, number, and size) did not differ significantly between *Pla2g5*$^{+/+}$ and *Pla2g5*$^{-/-}$ mice regardless of AT-II infusion (Fig. S6, *A–C*). Specifically, AT-II treatment increased various PE species and some PA species in plasma exosomes (Fig. S6, *D–H*). However, none of the phospholipid species (PC, PE, PA, PI, and PS) in plasma exosomes was affected by *Pla2g5* deficiency with or without AT-II infusion (Figs. S6, *D–H*). It is thus likely that, in the context of aortic dissection, sPLA$_2$-V retained on the endothelium hydrolyzes phospholipids mainly in membranes of AT-II-activated (or damaged) ECs, rather than those in circulating lipoproteins and exosomes, to release OA and LA.

OA and LA stabilize the aortic wall by up-regulating LOX expression

To address whether sPLA$_2$-V–driven fatty acids or their metabolites could affect LOX expression, we utilized human umbilical vein ECs (HUVECs) and human aortic VSMCs in culture. Consistent with the results of immunohistochemistry (Fig. 3*G* and Fig. S3*A*), *LOX* mRNA was mainly expressed in VSMCs, rather than in ECs, regardless of AT-II stimulation (Fig. 6*A*). *LOX* expression in VSMCs was increased ~4-fold after stimulation for 24 h with TGFβ1, a fibrogenic factor that is known to induce LOX (40) (Fig. 6*B*), whereas *LOX* expression in ECs was very low even after stimulation with TGFβ1 (Fig. 6*B*) or AT-II (Fig. 6*A*). Importantly, *LOX* expression in VSMCs was increased after culture with the conditioned medium of AT-II–stimulated but not control ECs, whereas this response was suppressed by a *PLA2G5*-specific siRNA, which blocked *PLA2G5* expression in ECs (Fig. 6, *C* and *D*), or by the sPLA$_2$ inhibitor varespladib (Fig. 6*E*). Although AT-II has been shown

Figure 3. Decreased LOX expression and function in aorta of AT-II–infused *Pla2g5*$^{-/-}$ mice. *A*, mRNA expression of LOX family members, vascular remodeling markers, and pro-inflammatory cytokines in the aortas of *Pla2g5*$^{+/+}$ and *Pla2g5*$^{-/-}$ mice with or without AT-II infusion for 48 h (n = 4–5). *B*, time course of *Lox* mRNA expression in the aortas of *Pla2g5*$^{+/+}$ and *Pla2g5*$^{-/-}$ mice after AT-II infusion (n = 3–8). Shown are immunoblotting of LOX protein, with GAPDH as an internal control (*C*), densitometric analysis of mature LOX protein relative to GAPDH (n = 3) (*D*), LOX activity (n = 4–5) (*E*), and insoluble/soluble collagen ratio (n = 3–4) (*F*) in the aortas of *Pla2g5*$^{+/+}$ and *Pla2g5*$^{-/-}$ mice with or without AT-II infusion for 48 h. *, $p < 0.05$; **, $p < 0.01$; *ns*, not significant by two-way ANOVA with Tukey's multiple-comparison test. Data are presented as mean ± S.E. (*error bars*) of the indicated number (n) of biological replicates (*A*, *B*, *D*, *E*, and *F*). *G*, immunofluorescence of aortas of *Pla2g5*$^{+/+}$ and *Pla2g5*$^{-/-}$ mice with or without AT-II infusion for 48 h using control IgG (*Ctrl*), anti-LOX antibody (*green*), and anti-CD31 antibody (*magenta*) with DAPI (*blue*). *Scale bars*, 20 μM. *H*, correlation of *PLA2G5* and *LOX* expression in human aorta (n = 12). Pearson correlation (r value) and statistical significance (p value) are indicated.

to activate cPLA$_2\alpha$ (41, 42) and cross-talks between sPLA$_2$-V and cPLA$_2\alpha$ in both directions have been reported (43–45), the increased *LOX* expression in VSMCs after culture with the conditioned medium of AT-II–stimulated ECs was not suppressed by AACOCF$_3$, a cPLA$_2\alpha$ inhibitor (Fig. 6*F*), implying that EC-derived sPLA$_2$-V contributes to LOX induction in VSMCs

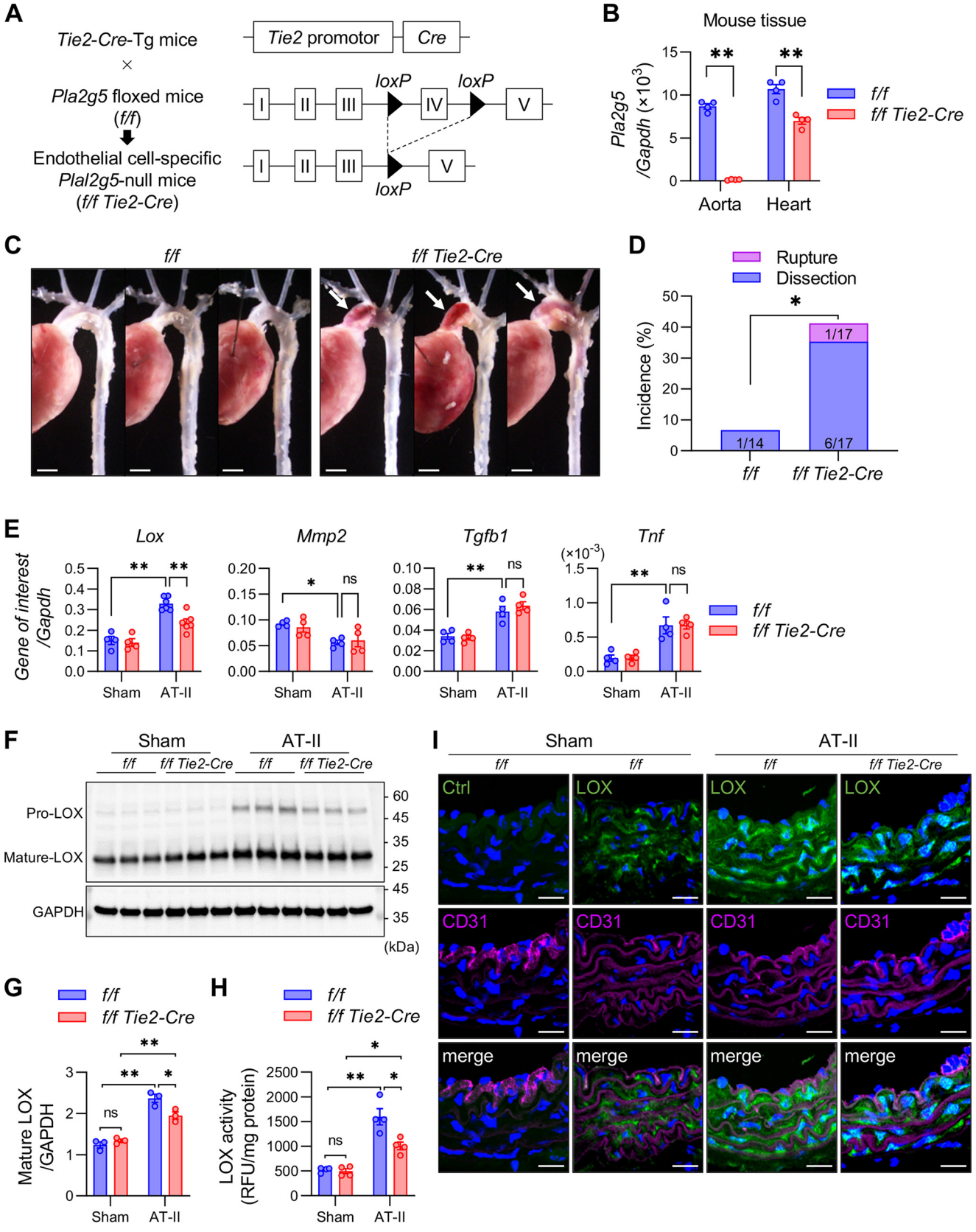

independently of cPLA$_2\alpha$. Furthermore, in the presence of TGFβ1, OA and LA, two major fatty acids released by sPLA$_2$-V, dose-dependently augmented *LOX* expression in VSMCs (Fig. 6*G*) and LOX activity in culture supernatant of VSMCs (Fig. 6*H*), although these fatty acids alone were ineffective. The *LOX*-inducing effect of OA or LA was more remarkable when the cells were treated with a suboptimal concentration of TGFβ1 (Fig. 6*I*). We also found that *TGFB1* was increased in ECs, but not in VSMCs, after stimulation for 24 h with AT-II (Fig. 6*J* and Fig S7 (*A* and *B*)). In addition, *TGFB1* was also increased in VSMCs after stimulation with TGFβ1 itself (Fig. 6*K*). It is thus likely that AT-II stimulation of ECs induces TGFβ1, which in turn increases LOX and TGFβ1 expression in VSMCs in paracrine and autocrine manners. However, the expression of *TGFB1* induced in both ECs and VSMCs (after stimulation with AT-II or TGFβ1, respectively) was not affected by OA or LA (Fig. 6, *J* and *K*).

In contrast to treatment of VSMCs with OA and LA, that with AA, EPA, or DHA decreased, rather than increased, the basal and TGFβ1-induced expression of *LOX* (Fig. S7*C*). Of the AA metabolites that were significantly altered in *Pla2g5*$^{-/-}$ mice (Fig. 5, *F* and *G*), PGE$_2$ suppressed both basal and TGFβ1-induced *LOX* expression, whereas LXA$_4$ had no effect (Fig. S7*D*). The two major sPLA$_2$-V–driven lysophospholipids, LPC and LPE, had no effect on the basal and TGFβ1-induced *LOX* expression in VSMCs (Fig. S7, *E* and *F*). Collectively, OA and LA, rather than HUFA metabolites and lysophospholipids, have the ability to increase TGFβ1-driven LOX expression in VSMCs. This again argues against the involvement of cPLA$_2\alpha$, which mobilizes AA selectively (41, 42), in the sPLA$_2$-V action in this situation.

In search of other factors that could affect sPLA$_2$-V expression in ECs, we found that *PLA2G5* was markedly up-regulated by TNFα, but not by VEGF (Fig. 6*L*). However, in the process of aortic dissection, the expression of *Tnf* was elevated (Fig. 3*A*), whereas that of *Pla2g5* was conversely decreased (Fig. 1*G*), after AT-II treatment. Therefore, it appears that there is no causal relationship between TNFα and sPLA$_2$-V in this disease. Conceivably, TNFα-induced sPLA$_2$-V expression may occur during atherosclerosis, where the expressions of both sPLA$_2$-V and TNFα are increased in the lesions (46).

It has been reported that TGFβ1 increases LOX expression through Smad and MAPK signaling (40). Indeed, phosphorylation of Smad2, Smad3, and p38 MAPK was increased in VSMCs after stimulation with TGFβ1, yet the addition of OA or LA did not influence their phosphorylation levels (Fig. S7*G*). As an alternative signaling pathway, TGFβ1 has the capacity to induce endoplasmic reticulum (ER) stress (47), and unsaturated fatty acids attenuate ER stress in general (48). Notably, the induction of various ER stress markers, including Bip protein (Fig. 6, *M* and *N*) as well as *BIP*, *ATF4*, *CHOP*, *ERdj4*, *EDEM1*, and *PDIA2* mRNAs (Fig. S7*H*), after stimulation for 24 h with TGFβ1 was significantly reduced by OA or LA supplementation.

ER stress has been reported to induce the expression of the transcription factor GATA3 (49), which has an inhibitory effect on LOX expression (50). Indeed, expression of *GATA3* was induced in VSMCs after stimulation for 24 h with TGFβ1 (Fig. 6*O*). This TGFβ1-induced expression of *GATA3* was reduced by the addition of OA or LA, and this reduction was reversed by the addition of thapsigargin (TGN), another ER stress inducer, although TGN alone did not affect the baseline level of *GATA3* expression (Fig. 6*O*). In the presence of TGFβ1, TGN canceled the *LOX*-inducing effect of OA and LA (Fig. 6*P*). Furthermore, *GATA3*-specific siRNAs, but not a nonsilencing control siRNA, which reduced both the baseline and the TGFβ1-induced *GATA3* expression (Fig. 6*Q*), reciprocally increased the TGFβ1-induced *LOX* expression (Fig. 6*R*). These results suggest that suppression of ER stress by OA or LA attenuates the induction of GATA3, thereby promoting the expression of LOX (Fig. 6*S*).

To address whether the action of OA or LA would be mediated by fatty acid receptors, such as the nuclear receptor PPARγ and the G protein–coupled receptor GPR40/120, we examined the effects of their synthetic agonists (rosiglitazone (RSG) and GW9508, respectively) on *LOX* expression in VSMCs. Unlike OA and LA (see above), the PPARγ and GPR40/120 agonists failed to increase the basal and TGFβ1-induced expression of *LOX* (Figs. S7, *I* and *J*), suggesting that the action of OA and LA is independent of these fatty acid receptors.

Increased susceptibility of Pla2g5$^{-/-}$ *mice to aortic dissection is rescued by OA- or LA-rich diet*

Finally, to examine whether exogenous supply of OA and LA could alter the sensitivity of *Pla2g5*$^{-/-}$ mice to aortic dissection *in vivo*, *Pla2g5*$^{-/-}$ mice fed an olive oil–rich diet (containing a high level of OA) or corn oil–rich diet (containing a high level of LA) for 2 weeks were subjected to AT-II infusion. Plasma levels of OA and/or LA, but not other fatty acids such as 16:0 (palmitic acid), 18:0 (stearic acid), 20:4 (AA), 20:5 (EPA), and 22:6 (DHA), were increased equally in both *Pla2g5*$^{+/+}$ and *Pla2g5*$^{-/-}$ mice fed an olive oil–rich or corn oil–rich diet compared with those fed a normal chow diet (Fig. S8*A*). Although LDL has been reported to down-regulate LOX (51), there were no differences in plasma levels of LDL and high-density lipoprotein, which were increased after feeding of an olive oil– or

Figure 4. Increased aortic dissection in EC-specific *Pla2g5*-null mice. *A*, schematic procedure for generation of EC-specific *Pla2g5*-null mice. *B*, expression of *Pla2g5* mRNA relative to *Gapdh* in the aorta and heart of control (*f/f*) and EC-specific *Pla2g5*-null (*f/f Tie2-Cre*) mice ($n = 4$). *C*, representative thoracic aortas of control and EC-specific *Pla2g5*-null mice after 7 days of AT-II infusion. *Arrows* indicate aortic dissection with intramural hematoma. *Scale bars*, 1 mm. *D*, incidence of thoracic aortic dissection or rupture in control ($n = 14$) and EC-specific *Pla2g5*-null ($n = 17$) mice within 7 days of AT-II infusion. *E*, mRNA expression of *Lox*, vascular remodeling markers (*Mmp2*, *Acta2*, and *Tgfb1*), and pro-inflammatory cytokine (*Tnf*) in the aortas of control and EC-specific *Pla2g5*-null mice with or without AT-II infusion for 48 h ($n = 4$–6). Shown are immunoblot analysis of LOX protein, with GAPDH as an internal control (*F*), densitometric analysis of mature LOX protein relative to GAPDH ($n = 3$) (*G*), and LOX activity ($n = 4$) (*H*) in the aortas of control and EC-specific *Pla2g5*-null mice with or without AT-II infusion for 48 h. *I*, immunofluorescence of aortas of control and EC-specific *Pla2g5*-null mice with or without AT-II infusion for 48 h using control IgG (*Ctrl*) or anti-LOX antibody (*green*) and anti-CD31 antibody (*magenta*) with DAPI (*blue*). *Scale bars*, 20 μm. *, $p < 0.05$; **, $p < 0.01$; *ns*, not significant by two-way ANOVA (*B*, *E*, *G*, and *H*) and by Fisher's exact test (*D*). Data are presented as mean ± S.E. (*error bars*) of the indicated number (*n*) of biological replicates.

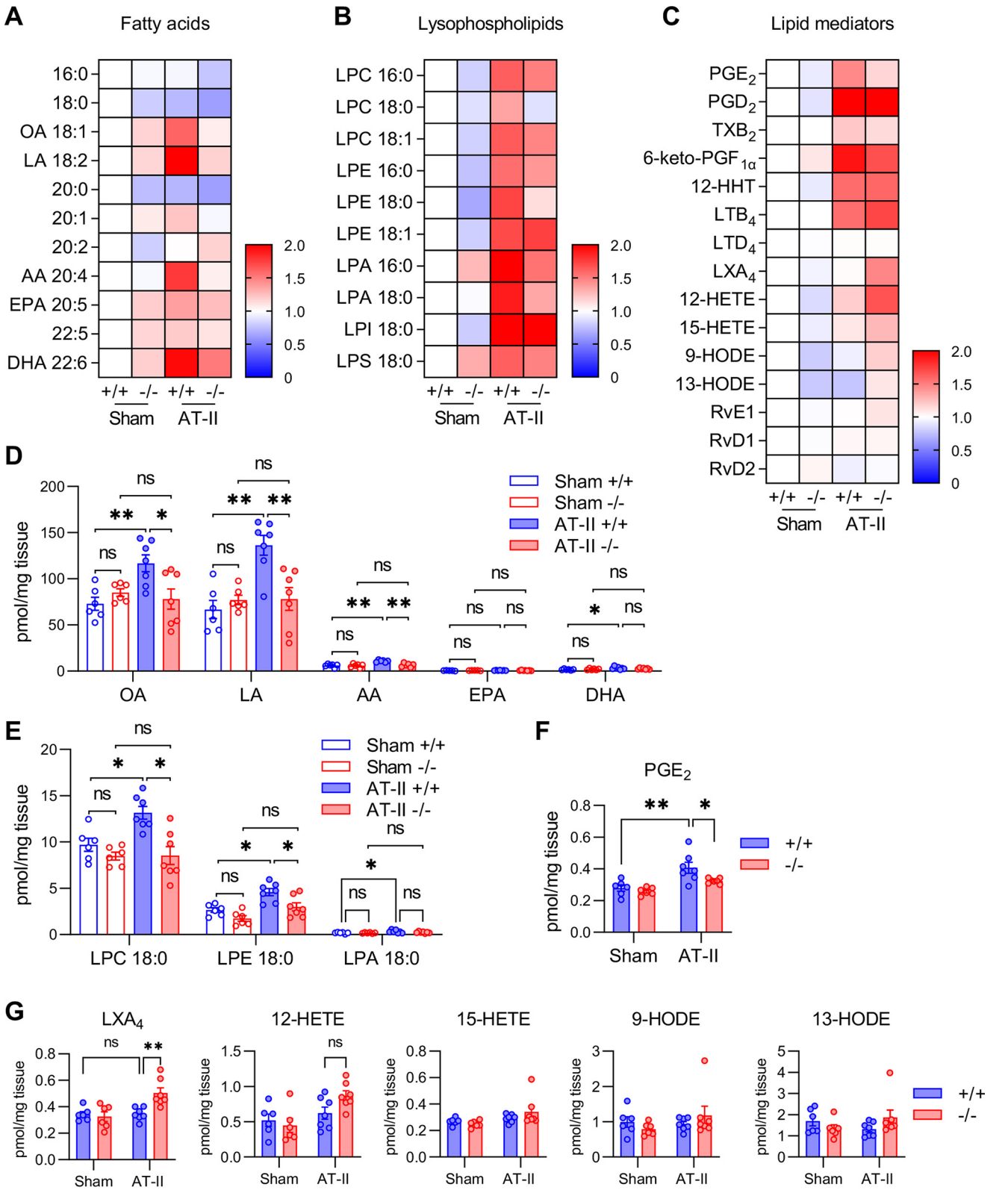

Figure 5. Altered lipid profiles in *Pla2g5*$^{-/-}$ mice after AT-II infusion. *A–C*, heat map representation of LC-ESI-MS/MS profiling of fatty acids (*A*), lysophospholipids (*B*), and lipid mediators (*C*) in the aortas of *Pla2g5*$^{+/+}$ and *Pla2g5*$^{-/-}$ mice with or without AT-II infusion for 12 h. -Fold changes relative to sham *Pla2g5*$^{+/+}$ are represented by *color* (n = 6–7). *D–G*, LC-ESI-MS/MS of unsaturated fatty acids (*D*), lysophospholipids (*E*), and HUFA-derived lipid mediators (*F* and *G*) presented as pmol/mg of tissue dry weight (n = 6–7). *, $p < 0.05$; **, $p < 0.01$; *ns*, not significant by two-way ANOVA followed by Tukey's multiple-comparison test. Data are presented as mean ± S.E. (*error bars*) of the indicated number (n) of biological replicates.

corn oil–rich diet, between both genotypes (Fig. S8*B*). Notably, under these conditions, *Pla2g5*$^{-/-}$ mice fed an olive oil– or corn oil–rich diet were fully protected from aortic dissection (Figs. 7, *A* and *B*). Furthermore, although aortic expression of *Lox* was lower and that of *Gata3* was higher in *Pla2g5*$^{-/-}$ mice than in *Pla2g5*$^{+/+}$ mice when a normal chow diet was supplied,

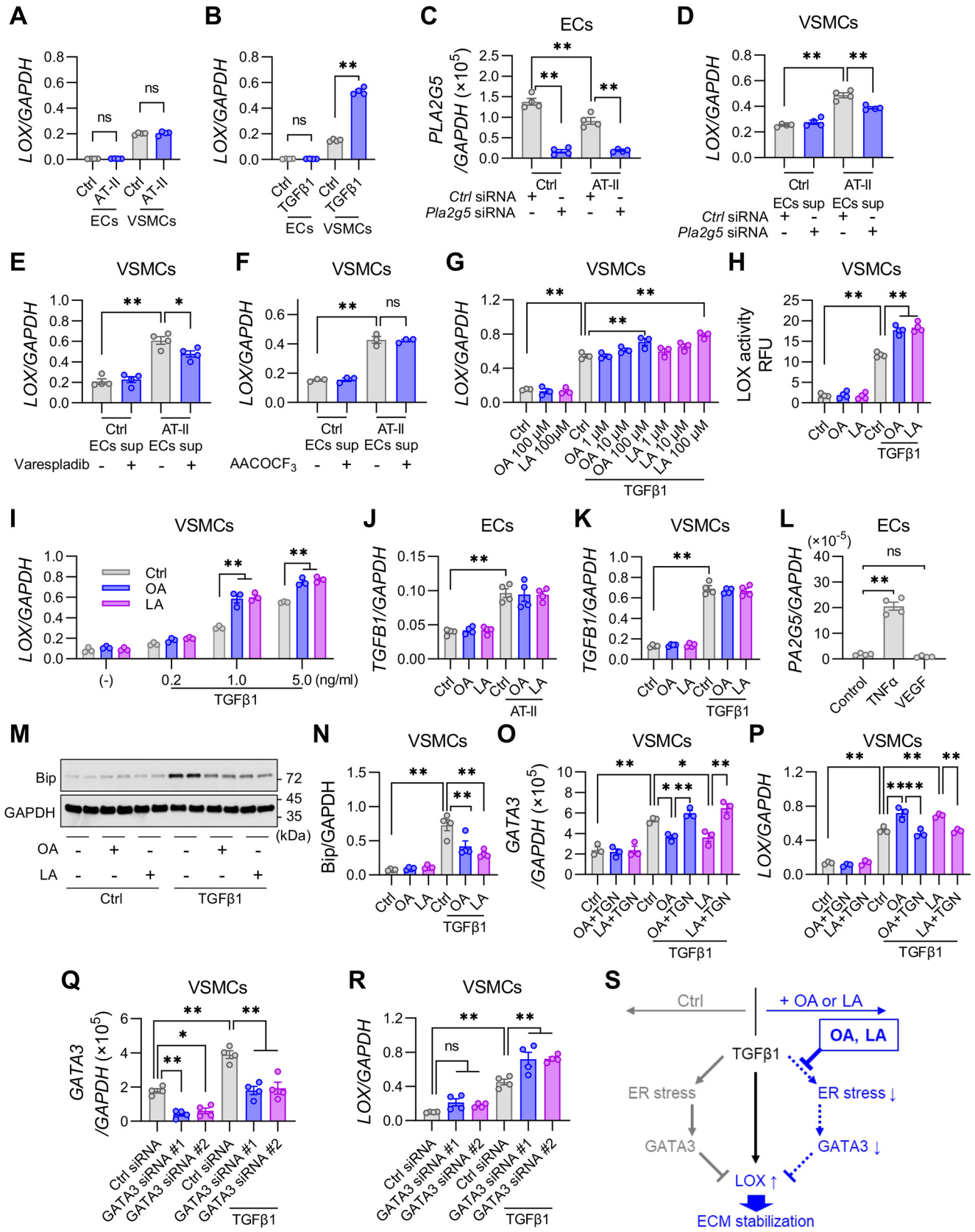

the expression of both in *Pla2g5*$^{-/-}$ mice was fully restored to levels similar to those in *Pla2g5*$^{+/+}$ mice after the olive oil– or corn oil–rich diet was supplied (Fig. 7, *C* and *D*). In contrast, *Pla2g5*$^{-/-}$ mice fed a cholesterol-rich, pro-atherogenic Western diet were as susceptible as those fed a chow diet to AT-II–induced aortic dissection (Fig. 7, *A* and *B*). Interestingly, aortic expression of *Pla2g5* was increased in mice fed an olive oil–rich diet relative to those fed a chow diet (Fig. 7*E*), implying a feed-forward amplification loop of the sPLA$_2$-V-OA pathway for the aortic stability. These findings collectively suggest that dietary supplementation of OA or LA could rescue the increased susceptibility of *Pla2g5*$^{-/-}$ mice to aortic dissection. Taken together, we conclude that aortic sPLA$_2$-V preferentially mobilizes OA and LA, which stabilize the extracellular matrix in the aortic wall by augmenting the AT-II–induced up-regulation of LOX, thereby exerting a protective effect against aortic dissection (Fig. 7*F*).

Discussion

Because of the paucity of preceding clinical signs (except for hypertension) and high mortality associated with aortic dissection and rupture, effective biomarkers that can predict aortic fragility and/or therapeutic targets for stabilization of the aortic wall are needed to mitigate against this life-threatening disease. However, the mechanisms underlying aortic dissection have remained obscure, largely due to the lack of a suitable animal model that mimics the pathology of this disease in humans. It is generally recognized that a Mediterranean diet is beneficial for cardiovascular health (12, 52). Olive oil, a key component of the Mediterranean diet, contains abundant OA, which has been proposed to be associated with reduced risks of cardiovascular disease and mortality (53), although understanding of the beneficial effect of this monounsaturated fatty acid is still incomplete. Herein, as a part of our ongoing attempts to clarify the biological roles of sPLA$_2$s using various sPLA$_2$-knockout mouse strains, we have demonstrated for the first time that OA as well as LA, mobilized endogenously from phospholipids by endothelial sPLA$_2$-V, plays a crucial role in stabilization of the aortic wall, thereby protecting against aortic dissection.

Previous studies have shown that sPLA$_2$-V is expressed in cardiomyocytes, IL-4–driven M2 macrophages, bronchial epithelial cells, and obesity-associated adipocytes, where it plays offensive or protective roles in myocardial infarction, atherosclerosis, asthma, and diet-induced obesity in accordance with disease contexts (17, 19, 28, 29, 43, 54). sPLA$_2$-V is also reportedly expressed in both mouse and human ECs (46, 55), and we have confirmed here that sPLA$_2$-V is indeed distributed almost exclusively in CD31-positive ECs within the aortic tissue, the expression level being far higher than those of other sPLA$_2$s. Thus, in addition to acting as a "metabolic sPLA$_2$" or an "asthmatic (or Th2-prone) sPLA$_2$" (28, 43), sPLA$_2$-V can be regarded as a major "endothelial sPLA$_2$" that controls vascular homeostasis and disease.

Reportedly, several (if not all) sPLA$_2$s, including sPLA$_2$-V, exhibit significant affinity for heparan sulfate proteoglycans on cell surfaces *in vitro* (32, 56), although *in vivo* evidence for this event has been lacking. We have demonstrated here that sPLA$_2$-V is retained on the luminal surface of the aortic endothelium and washed out after infusion of heparinized saline into the circulation, providing the first *in vivo* evidence for the heparin-binding behavior of sPLA$_2$-V. This view is reminiscent of sPLA$_2$-IIA, another heparin-binding sPLA$_2$ that is also released from heparan sulfate proteoglycans on EC surfaces into the circulation in heparinized patients (57). We previously reported that a heparin-binding sPLA$_2$, which is immunoreactive with an anti-sPLA$_2$-IIA antibody, is expressed in HUVECs (58), and based on the expression profile of sPLA$_2$s in ECs both *in vivo* and *in vitro*, it is likely that this heparin-binding sPLA$_2$ is attributed to sPLA$_2$-V rather than sPLA$_2$-IIA. Moreover, our results suggest that sPLA$_2$-V retained on aortic ECs mobilizes OA and LA from phospholipids (PC and PE) in AT-II–infused, but not AT-II–untreated, aortic cells in the process of aortic dissection, which also appears to be consistent with *in vitro* evidence that several sPLA$_2$s, including sPLA$_2$-V, act preferentially on the membranes of activated or damaged, rather than resting, cells (32, 56). In fact, the release of OA and LA by sPLA$_2$-V in aortic tissue is compatible with that in adipose tissue during diet-induced obesity (28) and in lung tissue during asthmatic inflammation (29) and is also consistent with the *in vitro* finding that it mobilizes OA from cultured cells (38). Thus, beyond the discovery of a novel role of this particular sPLA$_2$ in the aorta, our present study has provided a rationale for the action mode of sPLA$_2$ in an *in vivo* setting. Although sPLA$_2$-V has the capacity to hydrolyze phospholipids in

Figure 6. OA and LA attenuate ER stress and increase LOX expression in VSMCs. *A*, the expression of *LOX* relative to *GAPDH* in ECs and VSMCs treated for 24 h with or without AT-II (100 nM) ($n = 4$). *B*, the expression of *LOX* relative to *GAPDH* in ECs and VSMCs treated for 24 h with or without TGFβ1 (5 ng/ml) ($n = 4$). *C*, expression of *PLA2G5* in ECs that were pretreated with *PLA2G5*-specific siRNA or nonsilencing negative control siRNA and then treated for 24 h with or without AT-II ($n = 4$). *D–F*, expression of *LOX* in VSMCs treated for 24 h with the supernatant (*sup*) of ECs. *D*, ECs were pretreated with a *PLA2G5*-specific or control siRNA and then treated for 24 h with or without AT-II ($n = 4$). *E*, ECs were treated for 24 h with or without AT-II in the presence or absence of 100 nM varespladib, a pan-sPLA$_2$ inhibitor ($n = 4$). *F*, ECs were treated for 24 h with or without AT-II in the presence or absence of 10 μM AACOCF$_3$, a cPLA$_2\alpha$ inhibitor ($n = 3$). *G*, effect of OA or LA on the expression of *LOX* relative to *GAPDH* in VSMCs treated for 24 h with or without TGFβ1 ($n = 3$). *H*, LOX activity in supernatant of VSMCs treated for 24 h with or without TGFβ1 in the presence or absence of OA or LA (100 μM) ($n = 4$). *I*, expression of LOX in VSMCs treated for 24 h with or without TGFβ1 (0.2–5 ng/ml) in the presence or absence of OA or LA (100 μM) ($n = 4$). *J*, expression of *TGFB1* relative to *GAPDH* in ECs treated for 24 h with or without AT-II (100 nM) in the presence or absence of OA or LA (100 μM) ($n = 4$). *K*, expression of *TGFB1* in VSMCs treated for 24 h with or without TGFβ1 (5 ng/ml) in the presence or absence of OA or LA (100 μM) ($n = 4$). *L*, expression of *PLA2G5* in ECs treated for 24 h with or without TNFα (10 ng/ml) or VEGF (10 ng/ml) ($n = 4$). Shown are immunoblot analysis of Bip protein, with GAPDH as an internal control (*M*), and densitometric analysis of Bip protein relative to GAPDH ($n = 4$) (*N*) in VSMCs treated for 24 h with or without TGFβ1 in the presence (+) or absence (−) of OA or LA (100 μM). *O* and *P*, effect of OA or LA on the expression of *GATA3* (*O*) or *LOX* (*P*) in VSMCs treated for 24 h with or without TGFβ1 in the presence or absence of TGN (10 nM) ($n = 3$). *Q* and *R*, mRNA expression of *GATA3* (*Q*) and *LOX* (*R*) in VSMCs that were pretreated with *GATA3*-specific siRNAs (*#1* and *#2*) or control siRNA and then treated for 24 h with or without TGFβ1 ($n = 4$). *S*, a schematic summary of ECM stabilization by OA or LA in VSMCs. Whereas TGFβ1 induces LOX expression through canonical signaling pathways, it also induces ER stress leading to up-regulation of GATA3, which prevents LOX expression as a counter-regulatory arm. OA and LA counteract this process by attenuating TGFβ1-induced ER stress. *, $p < 0.05$; **, $p < 0.01$; *ns*, not significant by one-way ANOVA followed by Tukey's multiple-comparison test. Data are presented as mean ± S.E. (*error bars*) of the indicated number (*n*) of biological replicates.

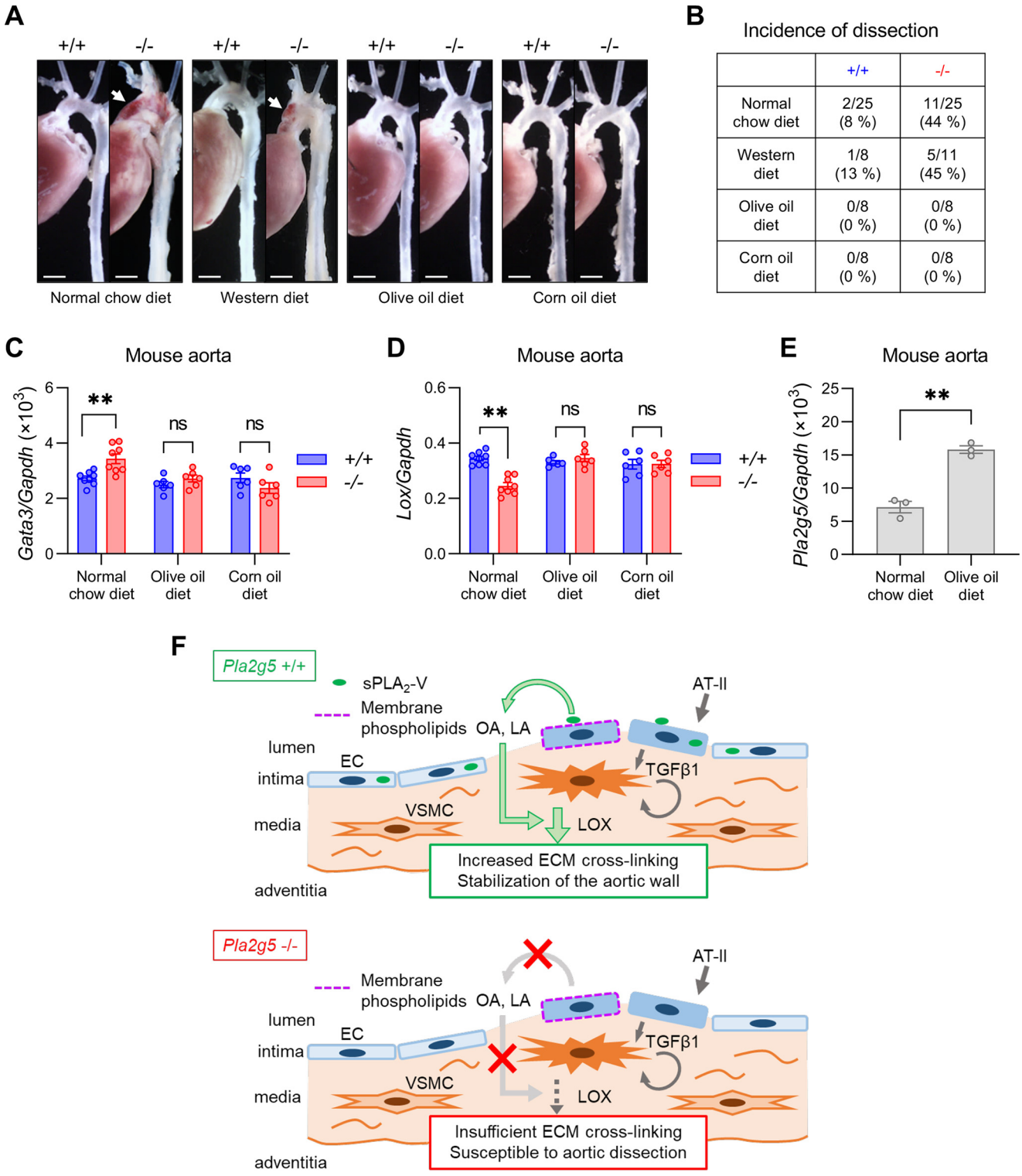

	+/+	-/-
Normal chow diet	2/25 (8 %)	11/25 (44 %)
Western diet	1/8 (13 %)	5/11 (45 %)
Olive oil diet	0/8 (0 %)	0/8 (0 %)
Corn oil diet	0/8 (0 %)	0/8 (0 %)

Figure 7. Exogenous supply of OA and LA protects against aortic dissection in *Pla2g5*$^{-/-}$ mice. *A*, representative photographs of thoracic aortas in *Pla2g5*$^{+/+}$ and *Pla2g5*$^{-/-}$ mice fed a normal chow diet, a Western diet, an olive oil–rich diet, or a corn oil–rich diet after 7 days of AT-II infusion. *Arrows*, aortic dissection with intramural hematoma. *Scale bars*, 1 mm. *B*, incidence of thoracic aortic dissection or rupture in *Pla2g5*$^{+/+}$ and *Pla2g5*$^{-/-}$ mice fed a normal chow diet ($n = 25$), a Western diet ($n = 8$–11), an olive oil–rich diet ($n = 8$), or a corn oil–rich diet ($n = 8$) within 7 days of AT-II infusion. *C* and *D*, mRNA expression of *Lox* (*C*) and *Gata3* (*D*) in the aortas of *Pla2g5*$^{+/+}$ and *Pla2g5*$^{-/-}$ mice after AT-II infusion for 48 h fed normal chow, an olive oil–rich diet, or a corn oil–rich diet ($n = 6$–8). *, $p < 0.05$; **, $p < 0.01$; *ns*, not significant by two-way ANOVA followed by Tukey's multiple-comparison test. *E*, *Pla2g5* expression in the aorta of *Pla2g5*$^{+/+}$ mice fed a normal chow or an olive oil–rich diet ($n = 3$). **, $p < 0.01$ by unpaired *t* test. Data are presented as mean ± S.E. (*error bars*) of the indicated number (*n*) of biological replicates. *F*, schematic diagram of the roles of endothelial sPLA$_2$-V in aortic stabilization. sPLA$_2$-V is a major sPLA$_2$ isoform expressed in aortic ECs and is largely retained on the luminal surface of the aortic endothelium likely through binding to heparan sulfate proteoglycans. Endothelial sPLA$_2$-V acts on membrane phospholipids of AT-II–activated ECs to mobilize OA and LA, which in turn promote AT-II–induced up-regulation of LOX that facilitates ECM cross-linking, thereby stabilizing the aortic wall. Impairment of this sPLA$_2$-V–driven lipid pathway leads to increased susceptibility to aortic dissection.

lipoproteins and microvesicles (*e.g.* exosomes) (28, 39), it is likely that the OA and LA released by sPLA$_2$-V are derived mainly from the membranes of AT-II–activated ECs, because blood cells and plasma in the aortic lumen were flushed out before sample preparation and because there were no alterations in lipid compositions in plasma lipoproteins and exosomes in *PLA2g5*$^{-/-}$ mice under the experimental conditions employed here. Nonetheless, the possibility that a minor fraction of these unsaturated fatty acids is liberated from lipoproteins and/or exosomes by endothelial sPLA$_2$-V cannot be fully ruled out and needs further elucidation. It is also possible that certain lipid molecules other than OA and LA would be additionally involved in the sPLA$_2$-V action.

LOX-mediated ECM stabilization plays a protective role against acute aortic dissection (35). Reportedly, LOX expression is promoted by fibrogenic factors such as TGFβ1 (40), whereas this process is counter-regulated by the transcription factor GATA3 (50). We have shown here that OA and LA, which are preferentially released by sPLA$_2$-V, attenuate ER stress, eventually leading to down-regulation of GATA3 and thereby up-regulation of LOX, thus revealing a functional interplay between phospholipid metabolism and ECM stabilization through the action of the endothelial sPLA$_2$. Considering that ECM stabilization is also important for the prevention of atherosclerotic plaque rupture, a major trigger of myocardial infarction (59, 60), the present finding that sPLA$_2$-V contributes to the stabilization of aortic ECM might account, at least partly, for the unfavorable result of the phase III clinical trial of varespladib, a pan-sPLA$_2$ inhibitor, which failed to show efficacy for the treatment of patients with cardiovascular diseases and in fact increased the risk of myocardial infarction (24). Specifically, whereas varespladib prevented atherosclerosis and aneurysm in animal models (19), it would increase the risk of aortic dissection through inhibiting sPLA$_2$-V and thus destabilize the vascular wall. Nonetheless, as varespladib inhibits various sPLA$_2$ isoforms in the group I/II/V/X branch (14–16), we do not rule out the possibility that this agent might have blocked another cardioprotective sPLA$_2$ isoform(s) or even another target(s) unrelated to sPLA$_2$ in the clinical study.

In contrast to our present study, Boyanovsky *et al.* (21) previously reported that sPLA$_2$-V promotes (rather than prevents) abdominal aortic aneurysm and rupture in response to AT-II infusion in mice with an *ApoE*$^{-/-}$ genetic background. *ApoE*$^{-/-}$ mice develop aortic dissection mainly in the supra-renal region of the abdominal aorta, where atherosclerotic lesions with chronic inflammation are evident at the origin of the celiac and mesenteric arteries as early as 6–8 weeks of age, and this may be followed by suprarenal abdominal aortic dissection in response to AT-II infusion (4, 5). Rosengren *et al.* (46) reported that sPLA$_2$-V is localized in macrophages and VSMCs in the atherosclerotic regions of *ApoE*- and *Ldlr*-double knockout mice. Conceivably, under the abnormal lipid profile and vascular inflammation resulting from *ApoE* or *Ldlr* deficiency (61, 62), the pro-inflammatory effects of some lipid metabolites driven by sPLA$_2$-V distributed in different cell types might become predominant, masking the protective effect of OA and LA mobilized by endothelial sPLA$_2$-V, although details of the underlying mechanism require further elucidation. Importantly, dissection is generally more common in the ascending aorta than in other aortic regions in humans, probably because of continuous exposure to the systolic jet from the left ventricle (3), which was also observed in our *Pla2g5*$^{-/-}$ mouse model. In this regard, administration of AT-II to *Pla2g5*$^{-/-}$ mice, independently of *ApoE* deletion, can be regarded as a groundbreaking mouse model of aortic dissection, having considerable potential for screening of effective treatments and/or diagnostic markers of this condition. Interestingly, regardless of the different outcomes of aortic rupture, Boyanovsky *et al.* also reported that sPLA$_2$-V increases the collagen content of atherosclerotic lesions (18), an event that seems to corroborate the LOX-inducing effect of sPLA$_2$-V demonstrated in the present study, again implying the ECM-stabilizing function of sPLA$_2$-V.

We have previously shown that sPLA$_2$-V has an offensive, rather than protective, role in a model of myocardial ischemia-reperfusion injury (43). In that model, the coronary artery is artificially ligated to induce myocardial injury. However, considering the pathological situation, myocardial infarction is induced by the occlusion due to plaque rupture in the coronary artery. The plaque rupture could be suppressed by the sPLA$_2$-V-LOX axis that may stabilize the fibrous cap (extracellular matrix) of the plaque. In the ischemia-reperfusion model, however, the protective effect of the sPLA$_2$-V-LOX axis may be bypassed by the artificial ligation of the coronary artery. Also, in the ischemia-reperfusion model, the contribution of sPLA$_2$-V expressed abundantly in cardiomyocytes and possibly in macrophages to the disease should be taken into account.

Last, it appears that our present findings have some relationships with previous studies describing the potential roles of sPLA$_2$s in cardiovascular homeostasis and diseases. Bernatchez *et al.* (63) reported that sPLA$_2$-V is expressed in HUVECs and involved in the synthesis of platelet-activating factor (a lysophospholipid-derived mediator) in response to VEGF, although we failed to observe the induction of sPLA$_2$-V by VEGF, and the role of sPLA$_2$-V in platelet-activating factor generation during aortic dissection remains to be elucidated. Consistent with our present study, Sonoki *et al.* demonstrated that sPLA$_2$-V is induced by TNFα and produces LPC in HUVECs (64) and also showed that an AT-II blocker inhibits TNFα-induced sPLA$_2$-V expression (65). It seems unlikely, however, that there is a functional interplay between sPLA$_2$-V and TNFα in aortic dissection, as described here. It has been shown that sPLA$_2$-IIA, when transgenically overexpressed in macrophages, induces collagen deposition in the atherosclerotic plaque (66), that AT-II induces the expression of sPLA$_2$-IIA in VSMCs (67), and that sPLA$_2$-IIA activates the LOX-mediated collagen pathway in myofibroblasts in the process of cardiac remodeling (68). These findings may indicate some functional redundancy between sPLA$_2$-V and -IIA in the context of cardiovascular disorders, although aortic dissection, arteriosclerosis, and cardiac remodeling are essentially different pathologies, and a direct comparison may not be appropriate.

In summary, our present study has revealed a novel lipid-driven mechanism controlling aortic stability, perturbation of which can be linked to aortic fragility and dissection. Central to this, sPLA$_2$-V plays a novel physiological role as a specific

sPLA$_2$ expressed spatiotemporally in aortic ECs by endogenously mobilizing the unsaturated fatty acids OA and LA as critical regulators of aortic LOX expression and thereby ECM stabilization. Our findings provide valuable insights into the functional link between phospholipid metabolism and aortic stabilization, thus contributing to the future development of novel diagnostic and/or therapeutic strategies for aortic dissection. Furthermore, our study might open a potential mechanism underlying the beneficial impact of the olive oil–rich (*i.e.* OA-rich) Mediterranean diet on cardiovascular health. Because there has been no clinical evidence for the relationship between corn oil–rich (*i.e.* LA-rich) diet and aortic dissection, the actual effect of corn oil–rich diet on this disease in humans should be carefully investigated in a future study.

Experimental procedures

Mice

Pla2g5$^{-/-}$, *Pla2g2d*$^{-/-}$, and *Pla2g2e*$^{-/-}$ mice, backcrossed onto a C57BL/6 background for more than 12 generations, were described previously (25, 28, 43). Heterozygous *Pla2g3*$^{+/-}$ mice (C57BL/6 × 129Sv) were backcrossed to the C57BL/6 background for three generations, and then male and female heterozygotes were intercrossed to obtain *Pla2g3*$^{-/-}$ mice and littermate *Pla2g3*$^{+/+}$ mice (25, 69). Mice expressing Cre recombinase under control of the *Tie2* gene promoter (*Tie2-Cre* transgenic mice) on the C57BL/6 background were purchased from Jackson Laboratory. Mice with a floxed allele in the *Pla2g5* gene (*Pla2g5*$^{flox/flox}$) (43) were crossed with *Tie2-Cre* Tg mice to generate EC-specific *Pla2g5*-null mice (*Pla2g5*$^{flox/flox}$; *Tie2-Cre*$^{Tg/+}$) and their littermate controls (*Pla2g5*$^{flox/flox}$; *Tie2-Cre*$^{+/+}$) (Fig. 4*A*). In all experiments, only male mice from 8 to 12 weeks of age (weight: 25–28 g) were used. All mice were housed in climate-controlled facilities at 25 ℃ with a 12-h light-dark cycle, with free access to standard laboratory food (CE2, CLEA) and water. All procedures were performed in accordance with approvals from the institutional animal care and use committees of the University of Yamanashi, the Tokyo Metropolitan Institute of Medical Science, and the University of Tokyo.

Animal models

Acute aortic dissection in mice was induced by subcutaneous infusion of AT-II (A9525, Sigma–Aldrich) for up to 7 days using a micro-osmotic pump (1007D, Alzet). Mice were anesthetized with inhaled isoflurane, and then micro-osmotic pumps were implanted through an incision in the midscapular region under sterile conditions. AT-II was dissolved in PBS and infused at 2 μg/kg/min. Sham animals underwent an identical surgical procedure, except that osmotic pumps containing PBS alone were implanted. As required, BAPN (A3134, Sigma–Aldrich), a LOX inhibitor, was administered for 3 days prior to AT-II treatment and continued for an additional 7 days concurrent with AT-II infusion. BAPN was dissolved in drinking water at a dose of 250 mg/100 ml or 500 mg/100 ml *ad libitum*. In some experiments, 8-week-old male mice were fed an OA-rich, LA-rich, or Western diet (Research Diets) for 2 weeks. The compositions of these diets are given in Table S1. Mice were observed at least twice a day, and an autopsy was performed immediately if any mice died during AT-II infusion. To harvest aortic tissues, mice were anesthetized with inhaled isoflurane, and then the abdominal and thoracic cavities were opened ventrally. After perfusion with saline through the left ventricle of the heart to remove blood, the aortic tissue was harvested carefully under a stereo microscope (SZ61, Olympus), as described previously (22).

Measurement of blood pressure

Blood pressure in mice was measured by a noninvasive tail-cuff method using a blood pressure device (BP-98A, Softron). Mice went through daily sessions of unrecorded measurements for several days to acclimate them to the procedure. Blood pressure was recorded before and 2 days after AT-II administration. For each mouse, an average of six consecutive measurements were taken.

Quantitative RT-PCR

Total RNA was extracted from tissues or cells using TRIzol reagent (Thermo Fisher Scientific). First-strand cDNA synthesis was performed using a ReverTra Ace qPCR RT Kit (Toyobo). PCRs were carried out using a TaqMan Gene Expression System (Applied Biosystems) on the 7500 Real-Time PCR System (Applied Biosystems). The probe and primer sets used are listed in Table S2.

Histological analysis

Aortas from mice were fixed in 4% (w/v) paraformaldehyde and embedded in paraffin, and then 5-μm-thick serial sections were prepared for HE or EVG staining. Digital images were acquired using a light microscope (BX41, Olympus).

Immunoblotting

Aortic tissues were isolated and homogenized in radioimmune precipitation buffer (Thermo Fisher Scientific) containing protease inhibitor mixture (Thermo Fisher Scientific) using TissueLyser II (Qiagen) with 7-mm stainless beads (Qiagen). The homogenates were centrifuged at 14,000 × *g* for 30 min at 4 ℃, and the supernatants were collected for immunoblotting. Tissue homogenates or cell lysates (10-μg protein equivalents) were subjected to SDS-PAGE on 10% (w/v) gels under reducing conditions. Protein concentrations were determined with a Bradford assay kit (Thermo Fisher Scientific). The separated proteins in the gels were electroblotted onto polyvinylidene difluoride membranes with a semi-dry blotter (Trans-Blot-Turbo, Bio-Rad). After blocking with polyvinylidene difluoride–blocking reagent (NYPBR01, Toyobo), the membranes were probed with primary antibodies at 1:2,000 dilution in Signal Enhancer HIKARI Solution A (02272-74, Nacalai Tesque) at room temperature for 2 h. Primary antibodies used in this study were as follows: rabbit antibody against LOX (ab174316) was from Abcam; rabbit antibody against Bip (#3177), p-Smad2 (#3108), Smad-2 (#5339), p-Smad3 (#9520), Smad3 (#9523), p-p38 MAPK (#4511), p38 MAPK (#8690), p-Akt (#4056), Akt (#9272), and GAPDH (#2118) were from Cell Signaling Technology. Then the membranes were then washed with TBS-T,

followed by incubation with horseradish peroxidase–conjugated anti-rabbit IgG (NA934, GE Healthcare) at 1:20,000 dilution in Signal Enhancer HIKARI Solution B (02297-64, Nacalai Tesque) for 1 h and then visualized using ECL Prime system (RPN2236, GE Healthcare). Images were visualized by LAS-4000 (GE Healthcare), and densitometric analysis was carried out using ImageJ software (National Institutes of Health). The whole blots are shown in Fig. S9.

Measurement of soluble/insoluble collagen

The amounts of soluble and insoluble (cross-linked) collagen in aortic tissues were measured using a Sircol collagen assay kit (S1000, S2000, Biocolor) in accordance with the manufacturer's protocol. Briefly, freeze-dried aortic tissues were weighed and incubated in dilute acid/pepsin solution with rotation overnight at 4 °C. The extracts were centrifuged, and the supernatants were collected as the cold acid/pepsin-soluble fraction. The insoluble fraction was extracted by digestion in acid solution at 65 °C for 3 h. The amounts of soluble and insoluble collagen were determined by a colorimetric reaction using Sircol dye (Sirius red dye). Collagen cross-linking was assessed as the ratio of insoluble to soluble collagen.

LOX activity assay

Aortic tissues were isolated and homogenized in 500 μl of 6 M urea in 0.02 M borate buffer (pH 8.0) using TissueLyser II (Qiagen) with 7-mm stainless beads. The homogenates were centrifuged at 14,000 × *g* for 30 min at 4 °C, and the supernatants were collected for the LOX activity assay. The activity was assessed using a lysyl oxidase activity assay kit (ab112139, Abcam) in accordance with the manufacturer's instructions and expressed as relative fluorescence units/mg of protein.

Gelatin zymography

Gelatinase activity in aortic tissue lysates was determined using a gelatin zymography kit (AK45, Primary Cell) in accordance with the manufacturer's instructions. Briefly, aortic tissues were homogenized in radioimmune precipitation buffer (Thermo Fisher Scientific) using TissueLyser II with 7-mm stainless beads and centrifuged at 14,000 × *g* for 30 min, and the supernatants were collected for the assay. Total protein (2.5-μg equivalent) was loaded onto gelatin-impregnated polyacrylamide gels and electrophoresed under nonreducing conditions. Then the gels were incubated in the enzymatic reaction buffer for 24 h at 37 °C. After incubation, the gels were stained with Coomassie Brilliant Blue, and then destained in methanol/acetate solution. The gels were scanned, and densitometric analysis was performed using ImageJ software.

Immunohistochemistry

Mouse or human aortic tissues were, snap-frozen in OCT compound and then sliced into 10-μm-thick sections. These sections were fixed with 4% paraformaldehyde for 5 min and then incubated with rabbit anti-sPLA$_2$-V polyclonal antibody (ab23709, Abcam), rabbit anti-LOX mAb (ab174316, Abcam), rabbit anti-LOX polyclonal antibody (ab31238, Abcam), rat anti-mouse CD31 mAb (550247, BD Biosciences), mouse anti-human CD31 mAb (M0823, Agilent), or rabbit anti-human sPLA$_2$-V polyclonal antibody, which did not cross-react with other sPLA$_2$s (70), or control antibody overnight at 4 °C. The sections were then treated with horseradish peroxidase–conjugated secondary antibody (Histofine Simple Stain MAX PO, Nichirei Biosciences) and visualized with diaminobenzidine (Vector Laboratory), followed by counterstaining with hematoxylin. For immunofluorescence, the sections treated with primary antibodies were incubated with secondary antibodies, including goat anti-rabbit IgG conjugated with Alexa Fluor 488 and goat anti-rat IgG conjugated with Alexa Fluor 594 (Thermo Fisher Scientific). Fluorescence images were acquired by a confocal microscope (FV-1000, Olympus).

Magnetic cell sorting (MACS) and flow cytometry analysis

Aortic tissues from five mice were excised, minced in Dulbecco's modified Eagle's medium (DMEM) (Thermo Fisher Scientific), and digested in 1 mg/ml collagenase type II (Worthington) solution with shaking for 30 min at 37 °C. The cell suspensions were then passed through 70-μm nylon cell strainers (Corning), and the cells were washed with MACS buffer (0.5% BSA and 2 mM EDTA in PBS). To isolate ECs, CD31 MicroBeads (130-097-418, Miltenyi Biotec) were used in accordance with the manufacturer's protocol. RNA extracted from the cells was taken for quantitative RT-PCR. For flow cytometry analysis, the cells were stained with phycoerythrin-conjugated anti-mouse CD31 antibody (130-102-608, Miltenyi Biotec) and analyzed using a cell analyzer (EC800, Sony Biotechnology). Dead cells were excluded using the viability dye Zombie Aqua (eBioscience).

LC-ESI-MS/MS

All procedures were performed as described previously (25, 71, 72). In brief, for detection of fatty acid oxygenated metabolites, lipids were extracted by using Sep-Pak C18 cartridges (Waters). Tissues were soaked in 10 volumes of methanol and homogenized with a Polytron homogenizer. After overnight incubation at −20 °C, water was added to the homogenates to give a final methanol concentration of 10% (v/v). The samples in 10% methanol were applied to the cartridges, washed with 10 ml of hexane, eluted with 3 ml of methyl formate, dried under N_2 gas, and dissolved in 60% methanol. As internal standards for determination of recovery, 50 pmol of d_4-labeled PGE$_2$ (Cayman Chemicals) was added to the samples. The analysis of fatty acid metabolites was performed using a 4000Q-TRAP quadrupole linear ion trap hybrid mass spectrometer (AB Sciex) with reverse-phase LC (LC-30AD; Shimadzu) combined with autosampler (SIL-30AC$_{MP}$; Shimadzu). The sample was applied to a Kinetex C18 column (2.1 × 150 mm, 1.7-μm particle; Phenomenex) coupled for ESI-MS/MS. The samples injected by the autosampler (10 μl) were directly introduced and separated by a step gradient with mobile phase A (water containing 0.1% acetic acid) and mobile phase B (acetonitrile/methanol = 4:1 (v/v)) at a flow rate of 0.2 ml/min and a column temperature of 45 °C.

For detection of fatty acids, phospholipids, and lysophospholipids, tissues were soaked in 10 volumes of 20 mM Tris-HCl (pH 7.4) and then homogenized with a Polytron homogenizer. Lipids were extracted by the method of Bligh and Dyer (73) and subjected to ESI-MS/MS using a 4000Q-TRAP and LC-30AD with a Kinetex C18 column, as described previously (71). As an internal standard, 50 pmol of d_5-labeled EPA (Cayman Chemicals), LPC (17:0), and PE (14:0-14:0) (Avanti Polar Lipids) were added to each sample. The samples were separated by a step gradient with mobile phase A (acetonitrile/methanol/water = 1:1:1 (v/v/v) containing 5 μM phosphoric acid and 1 mM ammonium formate) and mobile phase B (2-propanol containing 5 μM phosphoric acid and 1 mM ammonium formate) at a flow rate of 0.2 ml/min at 50 °C.

Identification was conducted using multiple-reaction monitoring transition and retention times, and quantification was performed based on peak area of the multiple-reaction monitoring transition and the calibration curve obtained using an authentic standard for each lipid (Table S3) (27, 71).

Evaluation of circulating exosomes

Mouse plasma exosomes were isolated using a total exosome isolation kit (4484450, Thermo Fisher Scientific) in accordance with the manufacturer's instructions. Analysis of particle numbers and sizes of plasma exosomes was performed by Theoria Science using a NanoSight nanoparticle-tracking system.

Analyses of plasma lipoproteins

Analysis of mouse plasma lipoproteins was performed by LipoSearch (Skylight Biotech).

Cell culture studies

HUVECs (EA.hy926), obtained from ATCC (CRL-2922), were cultured in DMEM supplemented with 10% (v/v) fetal bovine serum (FBS) and 50 μg/ml penicillin/streptomycin (P/S). Human aortic VSMCs (T/G HA-VSMCs), obtained from ATCC (CRL-1999), were cultured in Ham's F-12K medium (Thermo Fisher Scientific) supplemented with 10% FBS, 50 μg/ml P/S, 0.05 mg/ml ascorbic acid, 0.01 mg/ml insulin, 0.01 mg/ml transferrin, 10 ng/ml sodium selenite, and 0.03 mg/ml endothelial cell growth supplement (E2759, Sigma–Aldrich). Human fibroblasts (WI-38), obtained from ATCC (CCL-75), were cultured in DMEM supplemented with 10% FBS and 50 μg/ml P/S. For treatment, the cells were starved in serum-free DMEM containing 0.5% (w/v) fatty acid–free BSA (015-23871, Wako) for 24 h and then treated with or without 5 ng/ml TGFβ1, 10 ng/ml TNFα, or 10 ng/ml VEGF (all from R&D Systems) for 24 h. As required, the cells were treated with 1–100 μM OA, LA, AA, EPA, or DHA, 1 μM PGE_2, 1 μM LXA_4, 1–100 μM LPC (18:0), or 0.1–10 μM LPE (18:0) (Avanti Polar Lipids); 10 nM TGN, 0.1–10 μM RSG, or 0.1–10 μM GW9508 (GPR40/120 agonist) (all from Cayman Chemicals); 100 nM varespladib (Anthera Pharmaceuticals); or 10 μM $AACOCF_3$ (Cayman Chemicals). Fatty acids were mixed with fatty acid–free BSA at a 3.3:1 molar ratio and then diluted to the required concentration with culture media. Fatty acid-free BSA alone was used as an experimental control. In the gene knockdown experiments, ECs or VSMCs were transfected with *Pla2g5* siRNA (assay ID s10597), *GATA3* siRNA (assay ID 43432 or 106675, Thermo Fisher Scientific), or negative control siRNA (AM4611, Thermo Fisher Scientific) using Lipofectamine RNAiMAX (13778030, Thermo Fisher Scientific), in accordance with the manufacturer's instructions.

Human samples

Aortic tissues were obtained by curative resection from six patients (Asian, male sex, aged from 58 to 78 years), all of whom underwent aortic graft replacement surgically at the Yamanashi University Hospital (Yamanashi, Japan) from April 16, 2014 to December 31, 2019. The study was approved by the Ethics Committees of Yamanashi University (approval number 1801), with written informed consent from all patients. All studies involving human samples abide by the Declaration of Helsinki principles.

Statistical analysis

Results are expressed as mean ± S.E. Univariate comparison was performed with Fisher's exact test for categorical data. Differences between two groups were assessed by using an unpaired *t* test. Analysis of more than two groups was carried out either by one-way ANOVA or two-way ANOVA followed by Tukey post hoc comparison test. Survival curves were calculated by the Kaplan–Meier method and compared by the log-rank test. The association between variables was examined using Pearson correlation. GraphPad Prism (version 8.3.1) software was used to conduct statistical analyses.

Data availability

Data supporting the findings of this work are available within the paper and the supporting information. The raw data will be provided by the corresponding author upon request.

Author contributions—K. W. and M. M. conceptualization; K. W. resources; K. W., Y. T., and Y. M. data curation; K. W. formal analysis; K. W. and M. M. funding acquisition; K. W. validation; K. W., Y. T., and Y. M. investigation; K. W. methodology; K. W. writing-original draft; K. K. and M. M. supervision; M. M. writing-review and editing.

Funding and additional information—This work was supported by AMED-CREST Grant JP18gm0710006 and FORCE Grant JP19gm4010005 from the Japan Agency for Medical Research and Development (to M. M.) and Japan Society for the Promotion of Science KAKENHI Grants JP15H05905, JP16H02613, and JP18H05025 (to M. M.) and 25860591, 16K19436, and 19K07502 (to K. W.).

Conflict of interest—The authors declare that they have no conflicts of interest with the contents of this article.

Abbreviations—The abbreviations used are: AT-II, angiotensin II; AA, arachidonic acid; BAPN, β-aminopropionitrile; DHA, docosahexaenoic acid; ECM, extracellular matrix; EC, endothelial cell; HUVEC, human umbilical vein EC; EPA, eicosapentaenoic acid;

ER, endoplasmic reticulum; EVG, Elastica van Gieson; HE, hematoxylin and eosin; HETE, hydroxytetraenoic acid; HUFA, highly unsaturated fatty acid; LA, linoleic acid; ESI, electrospray ionization; LOX, lysyl oxidase; LPA, lysophosphatidic acid; LPC, lysophosphatidylcholine; LPE, lysophosphatidylethanolamine; LPI, lysophosphatidylinositol; LPS, lysophosphatidylserine; LXA_4, lipoxin A_4; MACS, magnetic cell sorting; MMP, matrix metalloproteinase; OA, oleic acid; PA, phosphatidic acid; PC, phosphatidylcholine; PE, phosphatidylethanolamine; PI, phosphatidylinositol; PS, phosphatidylserine; PGE_2, prostaglandin E_2; PLA_2, phospholipase A_2; $sPLA_2$, secreted PLA_2; $sPLA_2$-V, group V $sPLA_2$; $sPLA_2$-IIA, group IIA $sPLA_2$; $cPLA_2\alpha$, cytosolic $PLA_2\alpha$; TGN, thapsigargin; RSG, rosiglitazone; VSMC, vascular smooth muscle cell; p-, phosphorylated; GAPDH, glyceraldehyde-3-phosphate dehydrogenase; DMEM, Dulbecco's modified Eagle's medium; FBS, fetal bovine serum; P/S, penicillin/streptomycin; ANOVA, analysis of variance; DAPI, 4′,6-diamidino-2-phenylindole; MAPK, mitogen-activated protein kinase; LDL, low-density lipoprotein.

References

1. Nienaber, C. A., and Clough, R. E. (2015) Management of acute aortic dissection. *Lancet* **385,** 800–811 CrossRef
2. Mussa, F. F., Horton, J. D., Moridzadeh, R., Nicholson, J., Trimarchi, S., and Eagle, K. A. (2016) Acute aortic dissection and intramural hematoma: a systematic review. *JAMA* **316,** 754–763 CrossRef Medline
3. Nienaber, C. A., Clough, R. E., Sakalihasan, N., Suzuki, T., Gibbs, R., Mussa, F., Jenkins, M. P., Thompson, M. M., Evangelista, A., Yeh, J. S., Cheshire, N., Rosendahl, U., and Pepper, J. (2016) Aortic dissection. *Nat. Rev. Dis. Primers* **2,** 16053 CrossRef
4. Saraff, K., Babamusta, F., Cassis, L. A., and Daugherty, A. (2003) Aortic dissection precedes formation of aneurysms and atherosclerosis in angiotensin II-infused, apolipoprotein E-deficient mice. *Arterioscler. Thromb. Vasc. Biol.* **23,** 1621–1626 CrossRef Medline
5. Trachet, B., Aslanidou, L., Piersigilli, A., Fraga-Silva, R. A., Sordet-Dessimoz, J., Villanueva-Perez, P., Stampanoni, M. F. M., Stergiopulos, N., and Segers, P. (2017) Angiotensin II infusion into $ApoE^{-/-}$ mice: a model for aortic dissection rather than abdominal aortic aneurysm? *Cardiovasc. Res.* **113,** 1230–1242 CrossRef Medline
6. Coady, M. A., Rizzo, J. A., and Elefteriades, J. A. (1999) Pathologic variants of thoracic aortic dissections. Penetrating atherosclerotic ulcers and intramural hematomas. *Cardiol. Clin.* **17,** 637–657 CrossRef Medline
7. Son, B. K., Sawaki, D., Tomida, S., Fujita, D., Aizawa, K., Aoki, H., Akishita, M., Manabe, I., Komuro, I., Friedman, S. L., Nagai, R., and Suzuki, T. (2015) Granulocyte macrophage colony-stimulating factor is required for aortic dissection/intramural haematoma. *Nat. Commun.* **6,** 6994 CrossRef Medline
8. Guo, D. C., Regalado, E. S., Gong, L., Duan, X., Santos-Cortez, R. L., Arnaud, P., Ren, Z., Cai, B., Hostetler, E. M., Moran, R., Liang, D., Estrera, A., Safi, H. J., Leal, S. M., *et al.* (2016) LOX mutations predispose to thoracic aortic aneurysms and dissections. *Circ. Res.* **118,** 928–934 CrossRef Medline
9. Lee, V. S., Halabi, C. M., Hoffman, E. P., Carmichael, N., Leshchiner, I., Lian, C. G., Bierhals, A. J., Vuzman, D., Mecham, R. P., Frank, N. Y., and Stitziel, N. O. (2016) Loss of function mutation in LOX causes thoracic aortic aneurysm and dissection in humans. *Proc. Natl. Acad. Sci. U.S.A.* **113,** 8759–8764 CrossRef Medline
10. Kurihara, T., Shimizu-Hirota, R., Shimoda, M., Adachi, T., Shimizu, H., Weiss, S. J., Itoh, H., Hori, S., Aikawa, N., and Okada, Y. (2012) Neutrophil-derived matrix metalloproteinase 9 triggers acute aortic dissection. *Circulation* **126,** 3070–3080 CrossRef Medline
11. Kimura, T., Shiraishi, K., Furusho, A., Ito, S., Hirakata, S., Nishida, N., Yoshimura, K., Imanaka-Yoshida, K., Yoshida, T., Ikeda, Y., Miyamoto, T., Ueno, T., Hamano, K., Hiroe, M., Aonuma, K., *et al.* (2014) Tenascin C protects aorta from acute dissection in mice. *Sci. Rep.* **4,** 4051 CrossRef Medline
12. Estruch, R., Ros, E., Salas-Salvadó, J., Covas, M. I., Corella, D., Arós, F., Gómez-Gracia, E., Ruiz-Gutiérrez, V., Fiol, M., Lapetra, J., Lamuela-Raventos, R. M., Serra-Majem, L., Pintó, X., Basora, J., Muñoz, M. A., *et al.* (2018) Primary prevention of cardiovascular disease with a Mediterranean diet supplemented with extra-virgin olive oil or nuts. *N. Engl. J. Med.* **378,** e34 CrossRef Medline
13. Murakami, M., Sato, H., Miki, Y., Yamamoto, K., and Taketomi, Y. (2015) A new era of secreted phospholipase A_2. *J. Lipid Res.* **56,** 1248–1261 CrossRef Medline
14. Kugiyama, K., Ota, Y., Takazoe, K., Moriyama, Y., Kawano, H., Miyao, Y., Sakamoto, T., Soejima, H., Ogawa, H., Doi, H., Sugiyama, S., and Yasue, H. (1999) Circulating levels of secretory type II phospholipase A_2 predict coronary events in patients with coronary artery disease. *Circulation* **100,** 1280–1284 CrossRef Medline
15. Kugiyama, K., Ota, Y., Sugiyama, S., Kawano, H., Doi, H., Soejima, H., Miyamoto, S., Ogawa, H., Takazoe, K., and Yasue, H. (2000) Prognostic value of plasma levels of secretory type II phospholipase A_2 in patients with unstable angina pectoris. *Am. J. Cardiol.* **86,** 718–722 CrossRef Medline
16. Mallat, Z., Steg, P. G., Benessiano, J., Tanguy, M. L., Fox, K. A., Collet, J. P., Dabbous, O. H., Henry, P., Carruthers, K. F., Dauphin, A., Arguelles, C. S., Masliah, J., Hugel, B., Montalescot, G., Freyssinet, J. M., *et al.* (2005) Circulating secretory phospholipase A_2 activity predicts recurrent events in patients with severe acute coronary syndromes. *J. Am. Coll. Cardiol.* **46,** 1249–1257 CrossRef Medline
17. Bostrom, M. A., Boyanovsky, B. B., Jordan, C. T., Wadsworth, M. P., Taatjes, D. J., de Beer, F. C., and Webb, N. R. (2007) Group V secretory phospholipase A_2 promotes atherosclerosis: evidence from genetically altered mice. *Arterioscler. Thromb. Vasc. Biol.* **27,** 600–606 CrossRef Medline
18. Boyanovsky, B., Zack, M., Forrest, K., and Webb, N. R. (2009) The capacity of group V $sPLA_2$ to increase atherogenicity of $ApoE^{-/-}$ and $LDLR^{-/-}$ mouse LDL *in vitro* predicts its atherogenic role *in vivo*. *Arterioscler. Thromb. Vasc. Biol.* **29,** 532–538 CrossRef Medline
19. Fraser, H., Hislop, C., Christie, R. M., Rick, H. L., Reidy, C. A., Chouinard, M. L., Eacho, P. I., Gould, K. E., and Trias, J. (2009) Varespladib (A-002), a secretory phospholipase A_2 inhibitor, reduces atherosclerosis and aneurysm formation in $ApoE^{-/-}$ mice. *J. Cardiovasc. Pharmacol.* **53,** 60–65 CrossRef Medline
20. Zack, M., Boyanovsky, B. B., Shridas, P., Bailey, W., Forrest, K., Howatt, D. A., Gelb, M. H., de Beer, F. C., Daugherty, A., and Webb, N. R. (2011) Group X secretory phospholipase A_2 augments angiotensin II-induced inflammatory responses and abdominal aortic aneurysm formation in apoE-deficient mice. *Atherosclerosis* **214,** 58–64 CrossRef Medline
21. Boyanovsky, B. B., Bailey, W., Dixon, L., Shridas, P., and Webb, N. R. (2012) Group V secretory phospholipase A_2 enhances the progression of angiotensin II-induced abdominal aortic aneurysms but confers protection against angiotensin II-induced cardiac fibrosis in apoE-deficient mice. *Am. J. Pathol.* **181,** 1088–1098 CrossRef Medline
22. Watanabe, K., Fujioka, D., Saito, Y., Nakamura, T., Obata, J. E., Kawabata, K., Watanabe, Y., Mishina, H., Tamaru, S., Hanasaki, K., and Kugiyama, K. (2012) Group X secretory PLA_2 in neutrophils plays a pathogenic role in abdominal aortic aneurysms in mice. *Am. J. Physiol. Heart Circ. Physiol.* **302,** H95–H104 CrossRef
23. Ait-Oufella, H., Herbin, O., Lahoute, C., Coatrieux, C., Loyer, X., Joffre, J., Laurans, L., Ramkhelawon, B., Blanc-Brude, O., Karabina, S., Girard, C. A., Payré, C., Yamamoto, K., Binder, C. J., Murakami, M., *et al.* (2013) Group X secreted phospholipase A_2 limits the development of atherosclerosis in LDL receptor-null mice. *Arterioscler. Thromb. Vasc. Biol.* **33,** 466–473 CrossRef Medline
24. Nicholls, S. J., Kastelein, J. J., Schwartz, G. G., Bash, D., Rosenson, R. S., Cavender, M. A., Brennan, D. M., Koenig, W., Jukema, J. W., Nambi, V., Wright, R. S., Menon, V., Lincoff, A. M., Nissen, S. E., and VISTA-16 Investigators (2014) Varespladib and cardiovascular events in patients with an acute coronary syndrome: the VISTA-16 randomized clinical trial. *JAMA* **311,** 252–262 CrossRef Medline

25. Miki, Y., Yamamoto, K., Taketomi, Y., Sato, H., Shimo, K., Kobayashi, T., Ishikawa, Y., Ishii, T., Nakanishi, H., Ikeda, K., Taguchi, R., Kabashima, K., Arita, M., Arai, H., Lambeau, G., *et al.* (2013) Lymphoid tissue phospholipase A_2 group IID resolves contact hypersensitivity by driving antiinflammatory lipid mediators. *J. Exp. Med.* **210,** 1217–1234 CrossRef Medline
26. Taketomi, Y., Ueno, N., Kojima, T., Sato, H., Murase, R., Yamamoto, K., Tanaka, S., Sakanaka, M., Nakamura, M., Nishito, Y., Kawana, M., Kambe, N., Ikeda, K., Taguchi, R., Nakamizo, S., *et al.* (2013) Mast cell maturation is driven via a group III phospholipase A_2-prostaglandin D_2-DP1 receptor paracrine axis. *Nat. Immunol.* **14,** 554–563 CrossRef Medline
27. Yamamoto, K., Miki, Y., Sato, M., Taketomi, Y., Nishito, Y., Taya, C., Muramatsu, K., Ikeda, K., Nakanishi, H., Taguchi, R., Kambe, N., Kabashima, K., Lambeau, G., Gelb, M. H., and Murakami, M. (2015) The role of group IIF-secreted phospholipase A_2 in epidermal homeostasis and hyperplasia. *J. Exp. Med.* **212,** 1901–1919 CrossRef Medline
28. Sato, H., Taketomi, Y., Ushida, A., Isogai, Y., Kojima, T., Hirabayashi, T., Miki, Y., Yamamoto, K., Nishito, Y., Kobayashi, T., Ikeda, K., Taguchi, R., Hara, S., Ida, S., Miyamoto, Y., *et al.* (2014) The adipocyte-inducible secreted phospholipases PLA2G5 and PLA2G2E play distinct roles in obesity. *Cell Metab.* **20,** 119–132 CrossRef Medline
29. Yamaguchi, M., Samuchiwal, S. K., Quehenberger, O., Boyce, J. A., and Balestrieri, B. (2018) Macrophages regulate lung ILC2 activation via Pla2g5-dependent mechanisms. *Mucosal Immunol.* **11,** 615–626 CrossRef Medline
30. Chen, J., Engle, S. J., Seilhamer, J. J., and Tischfield, J. A. (1994) Cloning and recombinant expression of a novel human low molecular weight Ca^{2+}-dependent phospholipase A_2. *J. Biol. Chem.* **269,** 2365–2368 Medline
31. Sawada, H., Murakami, M., Enomoto, A., Shimbara, S., and Kudo, I. (1999) Regulation of type V phospholipase A_2 expression and function by proinflammatory stimuli. *Eur. J. Biochem.* **263,** 826–835 CrossRef Medline
32. Murakami, M., Shimbara, S., Kambe, T., Kuwata, H., Winstead, M. V., Tischfield, J. A., and Kudo, I. (1998) The functions of five distinct mammalian phospholipase A_2s in regulating arachidonic acid release. Type IIa and type V secretory phospholipase A_2s are functionally redundant and act in concert with cytosolic phospholipase A_2. *J. Biol. Chem.* **273,** 14411–14423 CrossRef Medline
33. Tieu, B. C., Lee, C., Sun, H., Lejeune, W., Recinos, A., 3rd, Ju, X., Spratt, H., Guo, D. C., Milewicz, D., Tilton, R. G., and Brasier, A. R. (2009) An adventitial IL-6/MCP1 amplification loop accelerates macrophage-mediated vascular inflammation leading to aortic dissection in mice. *J. Clin. Invest.* **119,** 3637–3651 CrossRef Medline
34. Rodriguez, C., Martínez-González, J., Raposo, B., Alcudia, J. F., Guadall, A., and Badimon, L. (2008) Regulation of lysyl oxidase in vascular cells: lysyl oxidase as a new player in cardiovascular diseases. *Cardiovasc. Res.* **79,** 7–13 CrossRef Medline
35. Ren, W., Liu, Y., Wang, X., Jia, L., Piao, C., Lan, F., and Du, J. (2016) β-Aminopropionitrile monofumarate induces thoracic aortic dissection in C57BL/6 mice. *Sci. Rep.* **6,** 28149 CrossRef Medline
36. Mäki, J. M., Sormunen, R., Lippo, S., Kaarteenaho-Wiik, R., Soininen, R., and Myllyharju, J. (2005) Lysyl oxidase is essential for normal development and function of the respiratory system and for the integrity of elastic and collagen fibers in various tissues. *Am. J. Pathol.* **167,** 927–936 CrossRef Medline
37. Masuda, S., Murakami, M., Ishikawa, Y., Ishii, T., and Kudo, I. (2005) Diverse cellular localizations of secretory phospholipase A_2 enzymes in several human tissues. *Biochim. Biophys. Acta* **1736,** 200–210 CrossRef Medline
38. Balsinde, J., Balboa, M. A., Yedgar, S., and Dennis, E. A. (2000) Group V phospholipase A_2-mediated oleic acid mobilization in lipopolysaccharide-stimulated P388D_1 macrophages. *J. Biol. Chem.* **275,** 4783–4786 CrossRef Medline
39. Rousseau, M., Belleannee, C., Duchez, A. C., Cloutier, N., Levesque, T., Jacques, F., Perron, J., Nigrovic, P. A., Dieude, M., Hebert, M. J., Gelb, M. H., and Boilard, E. (2015) Detection and quantification of microparticles from different cellular lineages using flow cytometry. Evaluation of the impact of secreted phospholipase A_2 on microparticle assessment. *PLoS ONE* **10,** e0116812 CrossRef Medline
40. Voloshenyuk, T. G., Landesman, E. S., Khoutorova, E., Hart, A. D., and Gardner, J. D. (2011) Induction of cardiac fibroblast lysyl oxidase by TGF-β1 requires PI3K/Akt, Smad3, and MAPK signaling. *Cytokine* **55,** 90–97 CrossRef Medline
41. Khan, N. S., Song, C. Y., Jennings, B. L., Estes, A. M., Fang, X. R., Bonventre, J. V., and Malik, K. U. (2015) Cytosolic phospholipase $A_2\alpha$ is critical for angiotensin II-induced hypertension and associated cardiovascular pathophysiology. *Hypertension* **65,** 784–792 CrossRef Medline
42. Rao, G. N., Lassègue, B., Alexander, R. W., and Griendling, K. K. (1994) Angiotensin II stimulates phosphorylation of high-molecular-mass cytosolic phospholipase A_2 in vascular smooth-muscle cells. *Biochem. J.* **299,** 197–201 CrossRef Medline
43. Yano, T., Fujioka, D., Saito, Y., Kobayashi, T., Nakamura, T., Obata, J. E., Kawabata, K., Watanabe, K., Watanabe, Y., Mishina, H., Tamaru, S., and Kugiyama, K. (2011) Group V secretory phospholipase A_2 plays a pathogenic role in myocardial ischaemia-reperfusion injury. *Cardiovasc. Res.* **90,** 335–343 CrossRef Medline
44. Kikawada, E., Bonventre, J. V., and Arm, J. P. (2007) Group V secretory PLA_2 regulates TLR2-dependent eicosanoid generation in mouse mast cells through amplification of ERK and cPLA$_2\alpha$ activation. *Blood* **110,** 561–567 CrossRef Medline
45. Han, W. K., Sapirstein, A., Hung, C. C., Alessandrini, A., and Bonventre, J. V. (2003) Cross-talk between cytosolic phospholipase $A_2\alpha$ (cPLA$_2\alpha$) and secretory phospholipase A_2 (sPLA$_2$) in hydrogen peroxide-induced arachidonic acid release in murine mesangial cells: sPLA$_2$ regulates cPLA$_2\alpha$ activity that is responsible for arachidonic acid release. *J. Biol. Chem.* **278,** 24153–24163 CrossRef Medline
46. Rosengren, B., Peilot, H., Umaerus, M., Jönsson-Rylander, A. C., Mattsson-Hulten, L., Hallberg, C., Cronet, P., Rodriguez-Lee, M., and Hurt-Camejo, E. (2006) Secretory phospholipase A_2 group V: lesion distribution, activation by arterial proteoglycans, and induction in aorta by a Western diet. *Arterioscler. Thromb. Vasc. Biol.* **26,** 1579–1585 CrossRef Medline
47. Chen, C. A., Chang, J. M., Chang, E. E., Chen, H. C., and Yang, Y. L. (2018) Crosstalk between transforming growth factor-β1 and endoplasmic reticulum stress regulates α-smooth muscle cell actin expression in podocytes. *Life Sci.* **209,** 9–14 CrossRef Medline
48. Ishiyama, J., Taguchi, R., Akasaka, Y., Shibata, S., Ito, M., Nagasawa, M., and Murakami, K. (2011) Unsaturated FAs prevent palmitate-induced LOX-1 induction via inhibition of ER stress in macrophages. *J. Lipid Res.* **52,** 299–307 CrossRef Medline
49. Qiang, G., Kong, H. W., Fang, D., McCann, M., Yang, X., Du, G., Blüher, M., Zhu, J., and Liew, C. W. (2016) The obesity-induced transcriptional regulator TRIP-Br2 mediates visceral fat endoplasmic reticulum stress-induced inflammation. *Nat. Commun.* **7,** 11378 CrossRef Medline
50. Chu, I. M., Michalowski, A. M., Hoenerhoff, M., Szauter, K. M., Luger, D., Sato, M., Flanders, K., Oshima, A., Csiszar, K., and Green, J. E. (2012) GATA3 inhibits lysyl oxidase-mediated metastases of human basal triple-negative breast cancer cells. *Oncogene* **31,** 2017–2027 CrossRef Medline
51. Rodríguez, C., Raposo, B., Martínez-González, J., Casaní, L., and Badimon, L. (2002) Low density lipoproteins downregulate lysyl oxidase in vascular endothelial cells and the arterial wall. *Arterioscler. Thromb. Vasc. Biol.* **22,** 1409–1414 CrossRef Medline
52. Martínez-González, M. A., Gea, A., and Ruiz-Canela, M. (2019) The Mediterranean diet and cardiovascular health. *Circ. Res.* **124,** 779–798 CrossRef Medline
53. Guasch-Ferré, M., Hu, F. B., Martinez-González, M. A., Fitó, M., Bulló, M., Estruch, R., Ros, E., Corella, D., Recondo, J., Gómez-Gracia, E., Fiol, M., Lapetra, J., Serra-Majem, L., Muñoz, M. A., Pintó, X., *et al.* (2014) Olive oil intake and risk of cardiovascular disease and mortality in the PREDIMED study. *BMC Med.* **12,** 78 CrossRef Medline
54. Ohta, S., Imamura, M., Xing, W., Boyce, J. A., and Balestrieri, B. (2013) Group V secretory phospholipase A_2 is involved in macrophage activation and is sufficient for macrophage effector functions in allergic pulmonary inflammation. *J. Immunol.* **190,** 5927–5938 CrossRef Medline
55. López-Sagaseta, J., Puy, C., Tamayo, I., Allende, M., Cerveró, J., Velasco, S. E., Esmon, C. T., Montes, R., and Hermida, J. (2012) sPLA$_2$-V inhibits EPCR anticoagulant and antiapoptotic properties by accommodating

lysophosphatidylcholine or PAF in the hydrophobic groove. *Blood* **119,** 2914–2921 CrossRef Medline

56. Murakami, M., Koduri, R. S., Enomoto, A., Shimbara, S., Seki, M., Yoshihara, K., Singer, A., Valentin, E., Ghomashchi, F., Lambeau, G., Gelb, M. H., and Kudo, I. (2001) Distinct arachidonate-releasing functions of mammalian secreted phospholipase A_2s in human embryonic kidney 293 and rat mastocytoma RBL-2H3 cells through heparan sulfate shuttling and external plasma membrane mechanisms. *J. Biol. Chem.* **276,** 10083–10096 CrossRef Medline
57. Nakamura, H., Kim, D. K., Philbin, D. M., Peterson, M. B., Debros, F., Koski, G., and Bonventre, J. V. (1995) Heparin-enhanced plasma phospholipase A_2 activity and prostacyclin synthesis in patients undergoing cardiac surgery. *J. Clin. Invest.* **95,** 1062–1070 CrossRef Medline
58. Murakami, M., Kudo, I., and Inoue, K. (1993) Molecular nature of phospholipases A_2 involved in prostaglandin I_2 synthesis in human umbilical vein endothelial cells. Possible participation of cytosolic and extracellular type II phospholipases A_2. *J. Biol. Chem.* **268,** 839–844 Medline
59. Ovchinnikova, O. A., Folkersen, L., Persson, J., Lindeman, J. H., Ueland, T., Aukrust, P., Gavrisheva, N., Shlyakhto, E., Paulsson-Berne, G., Hedin, U., Olofsson, P. S., and Hansson, G. K. (2014) The collagen cross-linking enzyme lysyl oxidase is associated with the healing of human atherosclerotic lesions. *J. Intern. Med.* **276,** 525–536 CrossRef Medline
60. Lusis, A. J. (2000) Atherosclerosis. *Nature* **407,** 233–241 CrossRef Medline
61. Getz, G. S., and Reardon, C. A. (2016) ApoE knockout and knockin mice: the history of their contribution to the understanding of atherogenesis. *J. Lipid Res.* **57,** 758–766 CrossRef Medline
62. Getz, G. S., and Reardon, C. A. (2016) Do the Apoe$^{-/-}$ and Ldlr$^{-/-}$ mice yield the same insight on atherogenesis? *Arterioscler. Thromb. Vasc. Biol.* **36,** 1734–1741 CrossRef Medline
63. Bernatchez, P. N., Winstead, M. V., Dennis, E. A., and Sirois, M. G. (2001) VEGF stimulation of endothelial cell PAF synthesis is mediated by group V 14 kDa secretory phospholipase A_2. *Br. J. Pharmacol.* **134,** 197–205 CrossRef Medline
64. Sonoki, K., Iwase, M., Sasaki, N., Ohdo, S., Higuchi, S., Takata, Y., and Iida, M. (2008) Secretory PLA_2 inhibitor indoxam suppresses LDL modification and associated inflammatory responses in TNFα-stimulated human endothelial cells. *Br. J. Pharmacol.* **153,** 1399–1408 CrossRef Medline
65. Sonoki, K., Iwase, M., Ohdo, S., Ieiri, I., Matsuyama, N., Takata, Y., and Kitazono, T. (2012) Telmisartan and *N*-acetylcysteine suppress group V secretory phospholipase A_2 expression in TNFα-stimulated human endothelial cells and reduce associated atherogenicity. *J. Cardiovasc. Pharmacol.* **60,** 367–374 CrossRef Medline
66. Ghesquiere, S. A., Gijbels, M. J., Anthonsen, M., van Gorp, P. J., van der Made, I., Johansen, B., Hofker, M. H., and de Winther, M. P. (2005) Macrophage-specific overexpression of group IIa $sPLA_2$ increases atherosclerosis and enhances collagen deposition. *J. Lipid Res.* **46,** 201–210 CrossRef Medline
67. Luchtefeld, M., Bandlow, N., Tietge, U. J., Grote, K., Pfeilschifter, J., Kaszkin, M., Beck, S., Drexler, H., and Schieffer, B. (2007) Angiotensin II type 1-receptor antagonism prevents type IIA secretory phospholipase A_2-dependent lipid peroxidation. *Atherosclerosis* **194,** 62–70 CrossRef Medline
68. Martin, R., Gutierrez, B., Cordova, C., Roman, A. S., Alvarez, Y., Hernandez, M., Cachofeiro, V., and Nieto, M. L. (2020) Secreted phospholipase A_2-IIA modulates transdifferentiation of cardiac fibroblast through EGFR transactivation: an inflammation-fibrosis link. *Cells* **9,** 396 CrossRef Medline
69. Murase, R., Taketomi, Y., Miki, Y., Nishito, Y., Saito, M., Fukami, K., Yamamoto, K., and Murakami, M. (2017) Group III phospholipase A_2 promotes colitis and colorectal cancer. *Sci. Rep.* **7,** 12261 CrossRef Medline
70. Degousee, N., Ghomashchi, F., Stefanski, E., Singer, A., Smart, B. P., Borregaard, N., Reithmeier, R., Lindsay, T. F., Lichtenberger, C., Reinisch, W., Lambeau, G., Arm, J., Tischfield, J., Gelb, M. H., and Rubin, B. B. (2002) Groups IV, V, and X phospholipases A_2s in human neutrophils: role in eicosanoid production and Gram-negative bacterial phospholipid hydrolysis. *J. Biol. Chem.* **277,** 5061–5073 CrossRef Medline
71. Yamamoto, K., Miki, Y., Sato, H., Murase, R., Taketomi, Y., and Murakami, M. (2017) Secreted phospholipase A_2 specificity on natural membrane phospholipids. *Methods Enzymol.* **583,** 101–117 CrossRef Medline
72. Yamamoto, K., Taketomi, Y., Isogai, Y., Miki, Y., Sato, H., Masuda, S., Nishito, Y., Morioka, K., Ishimoto, Y., Suzuki, N., Yokota, Y., Hanasaki, K., Ishikawa, Y., Ishii, T., Kobayashi, T., *et al.* (2011) Hair follicular expression and function of group X secreted phospholipase A_2 in mouse skin. *J. Biol. Chem.* **286,** 11616–11631 CrossRef Medline
73. Bligh, E. G., and Dyer, W. J. (1959) A rapid method of total lipid extraction and purification. *Can. J. Biochem. Physiol.* **37,** 911–917 CrossRef Medline